

Three-Dimensional Models of ACE and NEP Inhibitors and Their Use in the Design of Potent Dual ACE/NEP Inhibitors

Regine Bohacek,^{*,†} Stéphane De Lombaert,[†] Colin McMartin,[†] John Priestle,[‡] and Markus Grütter[‡]

Research Department, Pharmaceuticals Division, Ciba-Geigy Corporation, Summit, New Jersey 07901, and Department of Core Drug Discovery Technologies, Pharmaceuticals Division, Ciba-Geigy Ltd., Basel, Switzerland

Received March 13, 1995. Revised Manuscript Received January 18, 1996[⊗]

Abstract: A composite template for angiotensin converting enzyme (ACE, EC 3.4.15.1) inhibitors and a hypothetical model of the active site of neutral endopeptidase (NEP, EC 3.4.24.11) have been constructed and used to guide the design of dual ACE/NEP inhibitors. For the ACE template, a new computer program was used to flexibly superimpose potent, conformationally restricted ACE inhibitors. This program, which only considers the structures of the ligands, generated three possible templates. It was possible to evaluate the plausibility of these templates because new X-ray data is extending our knowledge of the binding of ligands to zinc metalloproteases. We have found that the available X-ray structures of inhibitors complexed to different zinc metalloproteases share certain conformational features. In each complex, the regions between the catalytic zinc and the P₁' side chain were found to have almost the same geometry. This geometry appears to be dictated by the mechanism of catalysis. Only one of the templates displays this geometry and is, therefore, proposed as a pharmacophore for ACE. To simulate NEP, we used the crystal structure of the active site of thermolysin (EC 3.4.24.4). These models of ACE and NEP predict that the conformation an inhibitor must adopt to bind to ACE differs from that required for binding to NEP. We have designed inhibitors in which conformationally restricted sections are linked by a flexible hinge, allowing the molecules to adapt to the conformation required by each enzyme. One of these inhibitors, a tricyclic α -thiol, **18** (CGS 28106), was found to inhibit both ACE and NEP with an IC₅₀ of 40 and 48 nM, respectively. The models predict that **18** binds to the S₁', S₂', and S₃' subsites of NEP and thermolysin and to the S₁, S₁', and S₂' subsites of ACE. The predicted mode of binding of **18** to thermolysin was experimentally verified by the determination of the X-ray crystal structure of the thermolysin/**18** complex. This is the first reported three-dimensional structure of an α -thiol bound to a zinc metalloprotease. Except for a single NEP inhibitor, the models we propose for ACE and NEP are able to differentiate between active and inactive compounds reported in the present as well as other studies of dual ACE/NEP inhibition.

Introduction

The vasoactive peptides angiotensin-II (Ang-II) and atrial natriuretic peptide (ANP) display opposing biological effects. The former stimulates vasoconstriction and sodium retention, while the latter produces vasodilation, diuresis, and natriuresis and decreases the levels of plasma renin and aldosterone.^{1–6} Therefore, a blockade of Ang-II production concomitant with a potentiation of endogenous ANP levels could represent a beneficial approach to the treatment of various cardiovascular disorders. Both peptides are regulated by distinct zinc metalloproteases. Angiotensin converting enzyme (ACE, EC.3.4.15.1) is a critical enzyme in the biosynthetic pathway of Ang-II. The use of ACE inhibitors is one of the most effective therapeutic approaches for the treatment of hypertension and congestive heart failure and underscores the physiological importance of this enzyme.⁷ On the other hand, neutral endopeptidase (NEP,

EC 3.4.24.11) has been implicated in the enzymatic inactivation of ANP *in vivo*.^{8,9} Inhibitors of this enzyme potentiate the biological properties of ANP and are currently being investigated clinically for their ability to induce ANP-like effects.¹⁰ More recently, preclinical results with combinations of ACE and NEP inhibitors have indicated possible synergistic effects.^{11–14} By exploiting some of the similarities between the two enzymes, we, and others, have been interested in combining both ACE and NEP inhibitory activities within a single chemical entity.^{15–21}

Both ACE and NEP are zinc metalloproteases with similar mechanism of action and, hence, some structural similarities. Although the three-dimensional structure of neither enzyme has

(7) Opie, L. H. *Angiotensin Converting Enzyme Inhibitors*; Wiley-Liss: New York, NY, 1992.

(8) Sonnenberg, J. L.; Sakane, Y. K.; Jeng, A. Y.; Koehn, J. A.; Ansell, J. A.; Wennogle, L. P.; Ghai, R. D. *Peptides* **1988**, *9*, 173–180.

(9) Kenny, A. J.; Stephenson, S. L. *FEBS Lett.* **1988**, *232*, 1–9.

(10) Richards, A. M.; Crozier, I. G.; Kosoglou, T.; Rallings, M.; Espiner, E. A.; Nicholls, M. G.; Yandle, T. G.; Ikram, H.; Frampton, C. *Hypertension* **1993**, *22*, 119–126.

(11) Margulies, K. B.; Perrella, M. A.; McKinley, L. J.; Burnett, J. C. *J. Clin. Invest.* **1991**, *88*, 1636–1642.

(12) Pham, I.; Gonzales, W.; El Amrani, A.-I. K.; Fournié-Zaluski, M.-C.; Philippe, M.; Laboulandine, I.; Roques, B. P.; Michel, J. B. *J. Pharmacol. Exp. Ther.* **1993**, *265*, 1339–1347.

(13) Seymour, A. A.; Asaad, M. M.; Lanoce, V. M.; Langenbacher, K. M.; Fennell, S. A.; Rogers, W. L. *J. Pharmacol. Exp. Ther.* **1993**, *266*, 872–883.

(14) Krulan, C.; Ghai, R. D.; Lappe, R. W.; Webb, R. L. *FASEB J.* **1993**, *7*, A247.

(15) Stanton, J. L.; Sperbeck, D. M.; Trapani, A. J.; Cote, D.; Sakane, Y.; Berry, C.; Ghai, R. D. *J. Med. Chem.* **1993**, *36*, 3829–3833.

(16) Fournié-Zaluski, M. C.; Coric, P.; Turcaud, S.; Rousselet, N.; Gonzalez, W.; Barbe, B. *J. Med. Chem.* **1994**, *37*, 1070.

* Corresponding author.

† Research Department.

‡ Department of Core Drug Discovery Technologies.

⊗ Abstract published in *Advance ACS Abstracts*, August 1, 1996.

(1) Brenner, B. M.; Ballerman, B. J.; Gunning, M. E.; Zeidel, M. L. *Physiol. Rev.* **1990**, *70*, 665–700.

(2) Bussien, J. P.; Biollaz, J.; Waeber, B.; Nussberger, J.; Turini, G. A.; Brunner, H. R.; Brunner-Feber, F.; Gomez, H. J.; Otterbein, E. S. *J. Cardiovasc. Pharmacol.* **1986**, *8*, 216–220.

(3) Lang, R. E.; Unger, T.; Ganten, D. *J. Hypertension* **1987**, *5*, 255–278.

(4) Needleman, P.; Blaine, E. H.; Greenwald, J. E.; Michener, M. L.; Saper, C. B. *Ann. Rev. Pharmacol. Toxicol.* **1989**, *29*, 23–54.

(5) Raine, A. E. G.; Firth, J. G.; Ledinham, J. G. G. *Clin. Sci.* **1989**, *76*, 1–8.

(6) Winquist, R. J.; Hintze, T. H. *Pharmacol. Ther.* **1990**, *48*, 417–426.

as yet been determined, the crystal structures of a significant number of zinc metalloproteases belonging to different families have been elucidated. Comparisons of the available structures in the next section reveal striking similarities as well as significant differences. Those regions of the enzymes where catalysis occurs are almost identical: the zinc, the zinc binding atoms, and the nearby catalytically important glutamic acid of each enzyme could readily be superimposed on the corresponding atoms of the other proteases. Most relevant to compound design, those regions of the inhibitor which mimic the scissile bond of the substrate also adopt a common conformation. However, beyond this region, the conformation that the inhibitor backbone and side chains adopt are significantly different. These differences reflect the variation in the shapes of the binding site of the different enzymes. These variations in binding site topology are responsible, at least in part, for the differences in substrate specificity.

ACE is a dipeptidyl carboxypeptidase usually cleaving the C-terminal dipeptide residue of its substrates. Potent ACE inhibitors have been designed to mimic both di- and tripeptides. Extensive structure activity studies of ACE inhibitors revealed three important structural features required for tight binding to ACE: a functional group acting as a zinc binder, an amido carbonyl group, and a C-terminal carboxylic acid.²²

NEP has a broader substrate specificity than ACE and can act both as an exopeptidase and as an endopeptidase.^{23–25} This behavior is reflected in the relatively large structural variations observed with NEP inhibitors. Some potent NEP inhibitors resemble tri- and tetrapeptides, while other smaller inhibitors are dipeptide mimics. The features critical for an NEP inhibitor include the following: a zinc binding group, a P₁' hydrophobic group, and an amide group (or amide surrogate) available for forming two hydrogen bonds. A terminal carboxylic acid group seems advantageous, although it is not essential nor is its precise position as critical as it is for ACE inhibitors.

Therefore, in order for a single molecule to inhibit both ACE and NEP, it must possess a zinc binding group. The atoms connecting this group to the rest of the inhibitor must be able to adopt the common conformation found in the zinc metalloprotease X-ray data. In addition, this molecule must include the functional groups required for tight binding to each enzyme, and these groups must be able to adopt the conformation appropriate for the different binding sites.

Conformational restriction is an attractive strategy to maximize the binding of an inhibitor to a specific active site by reducing the loss of conformational entropy experienced when a flexible molecule is removed from solvent and forced to fit into a binding site. However, at first glance, this approach does not appear suited for the design of dual inhibitors. Indeed, an inhibitor which is to efficiently occupy the binding sites of **two**

structurally different enzymes cannot be totally rigid. To overcome this problem, a molecule can be designed to include conformationally constrained sections designed to interact with certain areas in the binding site of each enzyme. These structural units can then be connected by a flexible hinge, allowing the entire molecule to adopt conformations complementary to the active site of each enzyme.

In this work we present a three-dimensional hypothesis of how inhibitors bind to ACE and to NEP. Since no actual or model structure of the binding site of ACE was available, we constructed a composite inhibitor template to model ACE inhibitors. For NEP we used the crystal structure of thermolysin. In our experience, a model of a binding site is more useful than an inhibitor template for compound design as the binding site contains information about both the allowed and forbidden space available to inhibitors. To construct a good inhibitor template, conformationally constrained potent inhibitors are necessary as well as considerable additional data to map out the binding site. Such information was available for ACE but not for NEP. However, at the conclusion of this work, we use the new dual inhibitor described here to construct an NEP inhibitor template which gives information about the P₁' and P₂' regions of NEP inhibitors.

The models developed in this work are consistent with the known structural data of different zinc metalloproteases. We show how the models were used to guide the design of potent, conformationally restricted dual inhibitors and conclude by testing the models with a wide variety of different inhibitors of ACE and NEP.

Structural Similarities of the Catalytic Sites of Zinc Metalloproteases. Zinc metalloproteases catalyze the hydrolysis of peptide bonds of protein substrates. The majority of these enzymes have a characteristic HEXXH motif and an additional conserved NEXXSD segment.²⁶ The first crystal structure which revealed these motifs was thermolysin.²⁷ In thermolysin, the two histidines of the motif are His¹⁴² and His¹⁴⁶ which bind to the zinc. The glutamic acid is Glu¹⁴³ proposed to be involved in the catalytic process. The glutamic acid found in the second segment is Glu¹⁶⁶ which is the third zinc binding residue. Carboxypeptidase A is a zinc-exopeptidase with a different zinc binding motif: HXXE. The histidine is His⁶⁹ and the glutamic acid Glu⁷². The third zinc binding residue is His¹⁹⁶, and the catalytically important glutamic acid is Glu²⁷⁰.²⁸

Recently, significant advances have been made in the structure determination of another family of zinc metalloproteases: the astacins,²⁹ the matrix metalloproteases,^{30–36} adamalysin II (snake

(17) Flynn, G. A.; Beight, D. W.; Mehdi, S.; Koelh, J. R.; Giroux, E. L.; French, J. F.; Hake, P. W.; Dage, R. C. *J. Med. Chem.* **1993**, *36*, 2420–1423.

(18) Roques, B. P. *Biochem. Soc. Trans.* **1993**, *21*, 678–685.

(19) Gros, C.; Noel, N.; Souque, A.; Schwartz, J. C.; Danvy, D.; Plaquevent, J. C.; Duhamel, L.; Duhamel, P.; Lecomte, J. M.; Bralet, J. *Proc. Natl. Acad. Sci. U.S.A.* **1991**, *88*, 4210–4214.

(20) Bhagwat, S. S.; Fink, C. A.; Gude, C.; Chan, K.; Qiao, Y.; Sakane, Y.; Berry, C.; Ghai, R. D. *Bioorg. Med. Chem. Lett.* **1994**, *4*, 2673–2676.

(21) De Lombaert, S.; Tan, J.; Stamford, L. J.; Sakane, Y.; Berry, C.; Ghai, R. D. *Bioorg. Med. Chem. Lett.* **1994**, *4*, 2715–2720.

(22) Wyvratt, M. J.; Patchett, A. A. *Med. Res. Rev.* **1985**, *5*, 483–531.

(23) Fournié-Zaluski, M.-C.; Soroca-Lucas, E.; Waksman, G.; Lhorens, C.; Schwartz, J.-C.; Roques, B. P. *Life Sci.* **1982**, *31*, 2947–2954.

(24) Gordon, E. M.; Cushman, D. W.; Tung, R.; Cheung, H. S.; Wang, F. L.; Delaney, N. G. *Life Sci.* **1983**, *33*, 113–116.

(25) Fournié-Zaluski, M.-C.; Lucas, E.; Waksman, G.; Roques, B. P. *Eur. J. Biochem.* **1984**, *139*, 267–274.

(26) Jongeneel, C. V.; Bouvier, J.; Bairoch, A. *FEBS Lett.* **1989**, *242*, 211–214.

(27) Colman, P. M.; Jansonius, J. N.; Matthews, B. W. *J. Mol. Biol.* **1972**, *70*, 701–724.

(28) Kester, W. R.; Matthews, B. W. *J. Biol. Chem.* **1977**, *252*, 7704–7710.

(29) Bode, W.; Gomis-Rueth, F.-X.; Huber, R.; Zwilling, R.; Stoeckler, W. *Nature* **1992**, *358*, 164–167.

(30) Lovejoy, B.; Cleasby, A.; Hassell, A. M.; Longley, K.; Luther, M. A.; Weigl, D.; McGeehan, G.; McElroy, A. B.; Drewry, D.; Lambert, M. H.; Jordan, S. R. *Science* **1994**, *263*, 375–377.

(31) Gooley, P. R.; O'Connell, J. F.; Marcy, A. I.; Cuca, G. C.; Salowe, S. P.; Bush, B. L.; Hermes, J. D.; Esser, C. K.; Hagmann, W. K.; Springer, J. P.; Johnson, B. A. *Struct. Biol.* **1994**, *1*, 111–118.

(32) Borkakoti, N.; Winkler, F. K.; Williams, D. H.; D'Arcy, A.; Broadhurst, M. J.; Brown, P. A.; Johnson, W. H.; Murray, E. J. *Struct. Biol.* **1994**, *1*, 106–110.

(33) Bode, W.; Reinemer, P.; Huber, R.; Kleine, T.; Schnierer, S.; Tschesche, H. *EMBO J.* **1994**, *13*, 1263–1269.

(34) Stams, T.; Spurlino, J. C.; Smith, D. L.; Wahl, R. C.; Ho, T. F.; Qoronfleh, M. W.; Banks, T. M.; Rubin, B. *Struct. Biol.* **1994**, *1*, 119–123.

(35) Becker, J. W.; Marcy, A. I.; Rokosz, L. L.; Axel, M. G.; Burbaum, J. J.; Fitzgerald, P. M. D.; Cameron, P. M.; Esser, C. K.; Hagmann, W. K.; Hermes, J. D.; Springer, J. P. *Protein Science* **1995**, *4*, 1966–1976.

venom metalloprotease),³⁷ and large bacterial zinc-endopeptidases such as serralsins.³⁸ (Bode et al. have suggested the name metzincins for this class of enzymes.³⁹) For all of these enzymes the HEXXH motif could be extended resulting in a longer consensus sequence HEXHXXGXXH. Upon solving the first X-ray structure of an enzyme belonging to this family (astacin), Bode et al. observed that the catalytic zinc, the active-site helix Tyr⁸⁶-Gly⁹⁹ and the zinc-liganding residues of astacin can be superimposed onto the corresponding portions of thermolysin.³⁹ Similarities between the binding sites of thermolysin with collagenase,³⁰ stromelysin,³⁵ and matrilysin³⁶ have also been noted. To date, the X-ray structures of all of the metzincins show that, despite low sequence homology, the zinc binding regions are almost identical and that these families of zinc metalloproteases show a similar overall fold.⁴⁰

The crystal structures of ACE and NEP have not as yet been determined. However, the primary sequences are known,^{41–43} and similarities to other zinc metalloproteases have been found. Both NEP and ACE have the consensus sequence HEXXH and EXXD. Devault et al. explored the differences between thermolysin and NEP using site-directed mutagenesis.^{44,45} The histidines (His⁵⁸³ and His⁵⁸⁷ in NEP) are two of the three zinc binding residues, and the glutamic acid of the second sequence (Glu⁵⁸⁴ in NEP) is the catalytically important glutamic acid. Fewer assignments have been proposed for the amino acids of ACE. However, the presence of the same consensus sequence supports the proposal that the active site(s) of this enzyme may also be similar to other zinc metalloproteases.¹⁸

Although the overall topology of thermolysin differs from carboxypeptidase A and both differ from the new “metzincins”, we wanted to see if there might be some structural similarity in the way potent inhibitors bind to these enzymes. Therefore, we superimposed the zinc and nearby atoms of the crystal structure of thermolysin complexed with ZF^PLA (4),⁴⁶ carboxypeptidase A complexed with ZFV^P(O)F (5),⁴⁷ collagenase complexed with 3,³⁰ and matrilysin complexed with 8.³⁶ (See the Experimental Section for details.) ZF^PLA and ZFV^P(O)F were selected because these are extremely potent inhibitors: ZF^PLA inhibits thermolysin with a $K_i = 68$ pM⁴⁸ and ZFV^P(O)F inhibits carboxypeptidase A with a $K_i = 11$ fM.⁴⁹ CLT (1) from the CLT/thermolysin crystal structure⁵⁰ and thiorphan (6) from the thiorphan/thermolysin crystal structure⁵¹ were also included because these inhibitors also inhibit ACE.^{52,53} Benzylsuccinic acid from its complex with thermolysin, 1HYT,⁵⁴ was added as a comparison to the matrilysin inhibitor. The

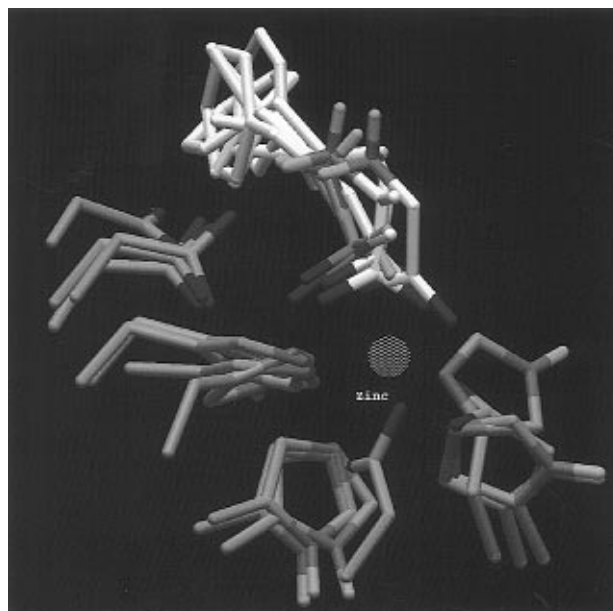


Figure 1. Superimposition of the zinc and nearby atoms of the crystal structure of thermolysin complexed with ZF^PLA (4), carboxypeptidase A complexed with ZFV^P(O)F (5), collagenase complexed with 3, and matrilysin complexed with 8. Thiorphan (6) and CLT (1) from the crystal structure of these inhibitors bound to thermolysin are also included. Enzyme carbon atoms are shown in gray, whereas inhibitor carbons are shown in white. Oxygens are depicted in red, nitrogen in blue, hydrogens in purple, phosphorus in green, and sulfur in yellow. The figure shows that the enzymes atoms near the zinc and the inhibitor atoms between the zinc and the P₁' side chains occupy a similar volume in each of these enzymes.

two matrix metalloproteases, collagenase and matrilysin, represent the metzincins family.

The resulting superimposition shown in Figure 1 reveals an interesting pattern. Even though these enzymes differ in the types of residues which bind to the zinc, the zinc as well as the enzyme atoms binding the zinc and the nearby catalytically important glutamic acid all occupy the same relative positions! In addition, even though these enzymes differ in their specificity, the inhibitor atoms between the zinc binding group and P₁' carbonyl side chain all occupy a common volume.

To compare the conformations adopted by inhibitors between the zinc and the P₂' side chain in the crystal structures of a large variety of enzyme/inhibitor complexes, three dihedral angles, X, Φ, and Ψ were measured. These angles are defined, and the values found are reported in Table 1. The first three inhibitors listed in Table 1 are most relevant to the subsequent discussion as these inhibitors are carboxyalkyl dipeptides like the ACE inhibitor benazeprilat⁵⁵ (14, see Figure 3). Two of these inhibitors are complexed to thermolysin, while the third is bound to collagenase. No complex of an analogous inhibitor bound to carboxypeptidase A is available. However, there is data available for three other inhibitors with a common succinyl moiety bound to carboxypeptidase A, thermolysin, and matrilysin. These are the last three inhibitors listed in Table 1.

(50) Monzinger, A. F.; Matthews, B. W. *Biochemistry* **1984**, *23*, 5724–5729.

(51) Roderick, S. L.; Fournié-Zaluski, B. P.; Roques, B. P.; Matthews, B. W. *Biochemistry* **1989**, *28*, 1493–1497.

(52) Maycock, A. L.; DeSousa, D. M.; Payne, L. G.; tenBroeke, J.; Wu, M. T.; Patchett, A. A. *Biochem. Biophys. Res. Commun.* **1981**, *102*, 963–969.

(53) Roques, B. P.; Lucas-Soroca, E.; Chaillet, P.; Costentin, J.; Fournié-Zaluski, M. *Proc. Natl. Acad. Sci. U.S.A.* **1983**, *80*, 3178–3182.

(54) Hausrath, A. C.; Matthews, B. W. *J. Biol. Chem.* **1994**, *269*, 18839–18842.

(55) Wathley, J. W. H.; Stanton, J. L.; Desai, M.; Babiars, J. E.; Finn, B. M. *J. Med. Chem.* **1985**, *28*, 1511–1516.

(36) Browner, M.; Smith, W.; Castelhano, A. *Biochemistry* **1995**, *34*, 660–6610.

(37) Gomis-Rueth, F. X.; Kress, L. F.; Kellermann, J.; Mayr, I.; Lee, X.; Huber, R.; Bode, W. *J. Mol. Biol.* **1994**, *239*, 513–544.

(38) Baumann, U.; Wu, S.; Flaherty, K. M.; McKay, D. B. *EMBO J.* **1993**, *12*, 3357–3364.

(39) Bode, W.; Gomis-Rueth, F.-X.; Stoeckler, W. *FEBS* **1993**, *331*, 134–140.

(40) Stoeckler, W.; Grams, F.; Baumann, U.; Reinemer, P.; Gomis-Rueth, F.; McKay, D. B.; Bode, W. *Protein Sci.* **1995**, *4*, 823–840.

(41) Devault, A.; Lazure, C.; Nault, C.; H., L.; Seidah, N. g.; Chretien, M.; Kahn, P.; Powell, J.; Mallet, J.; Beaumont, A.; Roques, B. P.; Crine, P.; Boileau, G. *EMBO J.* **1987**, *6*, 1317–13422.

(42) Malfroy, B.; Schofield, P. R.; Kuang, W.-J.; Seeburg, P. H.; Mason, A. J.; Henzel, W. J. *Biochem. Biophys. Res. Commun.* **1987**, *144*, 59–66.

(43) Soubrier, F.; Alhenc-Gelas, F.; Hubert, C.; Allegrini, J.; John, M.; Tregear, G.; Corvol, P. *Proc. Natl. Acad. Sci. U.S.A.* **1988**, *85*, 9386–9390.

(44) Devault, A.; Nault, C.; Zollinger, M.; Fournie-Zaluski, M. C.; Roques, B. P.; Crine, P.; Boileau, G. *J. Biol. Chem.* **1988**, *263*, 4033–4040.

(45) Devault, A.; Sales, N.; Nault, C.; Beaumont, A.; Roques, B. P.; Crine, P.; Boileau, G. *FEBS Lett.* **1988**, *231*, 54–58.

(46) Holden, H. M.; Tronrud, D. E.; Monzinger, A. F.; Weaver, L. H.; Matthews, B. W. *Biochemistry* **1987**, *26*, 8542–8553.

(47) Kim, H.; Lipscomb, W. N. *Biochemistry* **1991**, *30*, 8171–8180.

(48) Bartlett, P.; Marlowe, C. K. *Biochemistry* **1987**, *26*, 8553–8561.

(49) Kaplan, A. P.; Bartlett, P. *Biochemistry* **1991**, *30*, 8165–8170.

Table 1. Geometry of Zinc Ligand Groups Found in X-ray Structures of Zinc Metallo Protease/Inhibitor Complexes^f

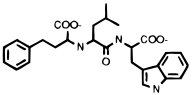
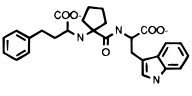
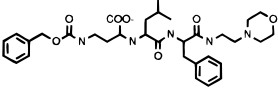
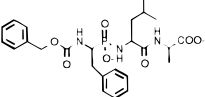
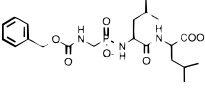
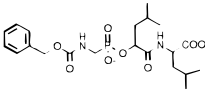
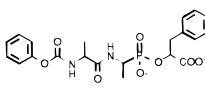
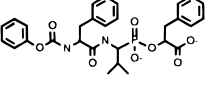
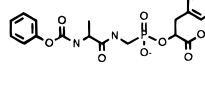
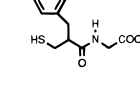
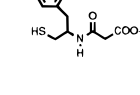
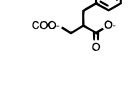
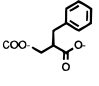
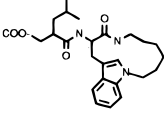
Enzyme	Structure Number	Inhibitor	Dihedral Angle X	Dihedral Angle Φ	Dihedral Angle Ψ	Resolution \AA	Zinc-Carboxylate Distances, \AA
Thermolysin 1TMN ⁵⁰	1		-26.6 ^a	-77.8	-40.9	1.9	2.0 2.4
Thermolysin 1THL ⁷⁰	2		-33.4 ^a	-75.5	-46.2	1.7	2.0 2.8
Collagenase 1CLG ³⁰	3		-50.0 ^a	-136.3	148.9	2.4	2.0 2.6
Thermolysin 4TMN ⁴⁶	4		-15.4 ^b	-85.5	-40.9	1.6	
Thermolysin 5TMN ⁴⁶			-21.5 ^b	-74.2	-39.3	1.6	
Thermolysin 6TMN ¹⁰⁸			-13.5 ^b	-82.0	-37.9	2.0	
Carboxypeptidase A 6CPA ¹⁰⁹			-8.7 ^c	-85.1	-28.6	2.0	
Carboxypeptidase A 7CPA ⁴⁷	5		-3.2 ^c	-76.8	-39.8	2.0	
Carboxypeptidase A 8CPA ⁴⁷			6.2 ^c	-87.7	-35.2	2.0	
Thermolysin Thiorphan ⁵¹	6		-35.2 ^d	-77.8	-54.4	1.7	
Thermolysin Retro-thiorphan ⁵¹	7		-62.1 ^d	-89.4	-140.7	1.7	
Thermolysin IHYT ⁵⁴			37.6 ^e	-77.9	-87.9	1.7	2.2 2.6

Table 1 (Continued)

Enzyme	Structure Number	Inhibitor	Dihedral Angles (degrees) X	Φ	Ψ	Resolution Å	Zinc-Carboxylate Distances, Å
Carboxypeptidase A 1CBX ¹¹⁰			18.4 ^e	-78.1	-46.6	2.0	2.3 2.6
Matrilysin 1MMQ ³⁶	8		17.7 ^e	-155.5	115.0	2.4	2.1 2.4

^a X: zinc-C(OO-)-N-CA; Φ : C(OO-)-N-CA-C(=O). ^b X: zinc-phosphorus-N-CA; Φ : phosphorus-N-CA-C(=O). ^c X: zinc-phosphorus-O-CA; Φ : phosphorus-O-CA-C(=O). ^d X: zinc-sulfur-CB-CA; Φ : sulfur-CB-CA-C(=O). ^e X: zinc-C(OO-)-CB-CA; Φ : carboxylate carbon-CB-CA-C(=O). ^f All Ψ dihedral angles are the angle between the P₁' α carbon and the P₁' carbonyl. For inhibitors with a terminal P₁' carboxylic acid, only the dihedral defining one of carboxylic oxygens is given.

Although not analogous to benazeprilat (the dihedral angles cannot be used directly as a comparison with any of the inhibitors used to construct the template), the close similarities found in the dihedral angles X and Φ of these last three inhibitors when binding to three significantly different enzymes again demonstrates the geometrical similarity of the catalytic site of all of these zinc metalloproteases.

Beyond the P₁' carbonyl, the similarities between the conformation adopted by the inhibitors of the different zinc metalloproteases ends. The significant differences between the dihedral angle Ψ of the thermolysin inhibitors with that of collagenase and matrilysin are shown in Table 1 (inhibitors of carboxypeptidase end with a P₁' carboxylic acid). The same is true of the P₁ and P₂ portions of the inhibitors. These differences reflect the different positions of the subsites of each enzyme responsible for the enzymes specificity. Several of the complete inhibitor structures are included in Figure 4B and show the regions where the inhibitors adopt similar as well as different conformations.

The X-ray structure of an inhibitor bound to neutrophil collagenase which does not occupy the S₁' and S₂' sites but instead binds to the S₁ and S₂ regions of the enzyme has also been reported.³³ The inhibitor, Pro-Leu-Gly-NHOH, has a weak binding affinity ($K_i = 4 \times 10^{-5}$ M) which may reflect the lack of favorable interactions which result from binding only to the solvent accessible unprimed regions of collagenase. The available X-ray data of zinc metalloproteases shows that it is the S₁' subsite of these enzymes which forms deep pockets offering solvent inaccessible hydrophobic regions for inhibitor binding.

In conclusion, the above considerations strongly suggests that when binding to ACE and NEP, the inhibitor will position the P₁' side chains into the S₁' enzyme subsite, and the regions between the inhibitor zinc binding group and the P₁' side chain will adopt the conformation found in the crystal structures of other zinc metalloprotease/inhibitor complexes. The remaining parts of the inhibitors are likely to be different, adopting the conformations required by each specific enzyme.

Model for ACE Inhibitors. The crystal structure of carboxypeptidase A was used to design some of the first ACE inhibitors. Scientists at Squibb developed a hypothetical model of the ACE active site based on carboxypeptidase A and used knowledge of carboxypeptidase A inhibitors in the design of captopril, **11** (see Figure 3).⁵⁶ However, when the design of ACE inhibitors was extended to *N*-carboxyalkyl analogs of captopril, resulting in enalaprilat, this model proved ineffectual as these types of inhibitors are poor carboxypeptidase inhibi-

tors.⁵⁷ Some of the *N*-carboxyalkyl dipeptides did inhibit thermolysin.⁵² The crystal structure of one such inhibitor, *N*-[1(*S*)-carboxy-3-phenylpropyl]-Leu-Trp (CLT, **1**), complexed to thermolysin was determined⁵⁰ and gave insight into the interactions such compounds form with the active site of zinc metalloproteases.⁵⁸ The crystal structure revealed that the Leu

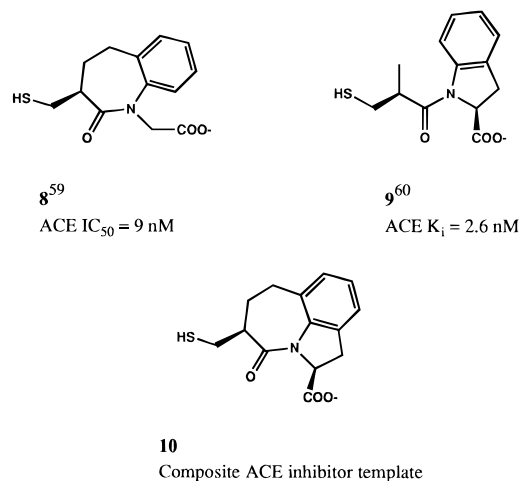


Figure 2. Two potent, conformationally restricted ACE inhibitors, **8** and **9**, were combined forming the original ACE inhibitor composite template **10**.

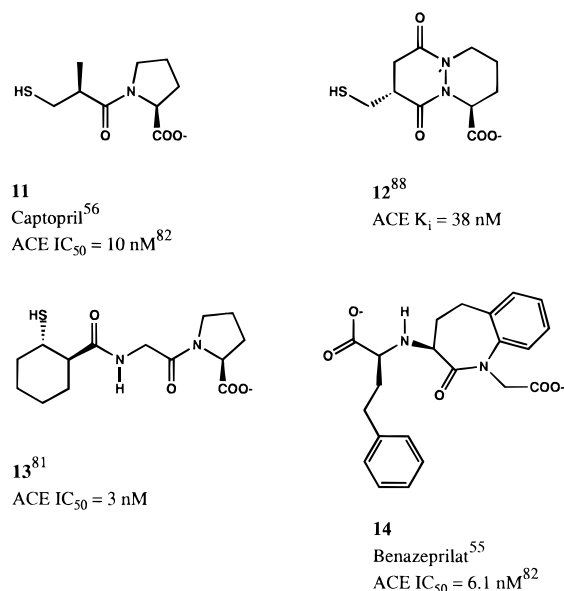


Figure 3. Four potent, conformationally restricted ACE inhibitors, **11**–**14**, were used to construct a composite ACE inhibitor template.

(56) Cushman, D. W.; Cheung, H. S.; Sabo, E. F.; Ondetti, M. A. *Biochemistry* **1977**, *16*, 5484–549.

Table 2. Characteristics of the Best Superimpositions Found by TFIT: Geometry of Benazeprilat and Captopril, Volume of the Four Superimposed Molecules, and Strain Energies of Each Inhibitor

template	dihedral angles (deg)			vol. ^c (Å ³)	strain energy ^d (kJ)			
	X ^a	Φ ^b	Ψ		11	12	13	14
Benazeprilat, 14								
1 ^e	-78.1	-98.4	-157.9	392.5	1	2	4	5
1-A	-78.1	-97.9	-158.1	394.2	4	2	4	5
2	32.1	-51.5	157.0	393.6	1	3	4	8
Captopril, 11								
1 ^e	-108.1	-64.4	124.8	392.5	1	2	4	5
1-A	99.6	-171.5	117.4	394.2	4	2	4	5
2	90.6	-65.3	125.0	393.6	1	3	4	8

All Ψ dihedral angles are the angle between the P₁' α carbon and the P₁' carbonyl. ^a X: for benazeprilat, zinc-carboxylate carbon-N-CA; for captopril, zinc-sulfur-CB-CA. ^b Φ: for benazeprilat, carboxylate carbon-N-CA-carbonyl; for captopril, sulfur-CB-CA-carbonyl. ^c The total volume of the four superimposed inhibitors. ^d The difference in energy between the global minimum and the energy of the conformation in the superimposition. ^e Superimposition predicted to be the bioactive conformation.

and Trp side chains of the inhibitor bind, respectively, to the S₁' and S₂' subsites of thermolysin. The Ala-Pro analog of this compound, *N*-[1(*S*)-carboxy-3-phenylpropyl]-Ala-Pro, a potent ACE inhibitor, was found to be a poor inhibitor of thermolysin⁵² indicating that the regions between S₁' and S₂' subsites as well as the S₂' subsite of thermolysin are not a good general model for the corresponding subsites of ACE.

As none of the available crystal structures make a good model for ACE, we decided on the following strategy: To determine the conformation of the side chains, we would use the structure of the inhibitors themselves to construct a template which would indicate the common energetically allowed positions various important inhibitor atoms could adopt. However, to determine the orientation close to the zinc, we would only accept a template displaying the same conformation as that found in the experimental X-ray data of zinc metalloproteases.

Initially, two potent, conformationally restricted ACE inhibitors previously discovered in our laboratories **8**^{59,60} were combined to form a three-dimensional ACE inhibitor composite template. (See Figure 2.) This template defines the P₁' and P₂' regions of the inhibitor. The initial template was used during the early phases of the project to model macrocyclic dual ACE/NEP inhibitors.⁶¹ When inhibitors were designed to incorporate residues designed to bind in the S₁ subsite, a more comprehensive template was required. Therefore, with the development of new computational methods for molecular superimposition, an expanded template was constructed.

Toward this goal, four potent, conformationally constrained inhibitors were selected (Figure 3). The criteria used to select the inhibitors were (1) strong binding to ACE (*K*_i less than 40 nM), (2) experimentally determined absolute configuration of the chiral centers, (3) variation in size, i.e., dipeptide and tripeptide mimics, and (4) conformational restriction of different parts of the molecule: the terminal carboxylic acid, the hydrophobic moieties, and the zinc-binding thiol.

Each inhibitor was constructed using the MACROMODEL molecular modeling program.⁶² The crystal structure of captopril⁶³ and benazeprilat⁶⁴ served as a starting point for the construction of these two molecules as well as inhibitor **13**. A zinc atom was connected to the metal binding group of each

inhibitor using the geometrical parameters obtained from X-ray crystal diffraction data both of small molecules⁶⁵ and enzyme/inhibitor complexes. Additional details are given in the Experimental Section.

To construct the inhibitor template, a computer program, TFIND,⁶⁶ was used to superimpose all four inhibitors. This program uses an extended force field potential which includes a superposition energy. Conformations of each molecule are identified that simultaneously have low internal strain energy and are aligned so that upon superimposition the match between atoms of similar type is optimized. Atoms are typed according to hydrophobicity, hydrogen bonding character, and formal charge (see Experimental Section). When the four ACE inhibitors were subjected to the TFIND program, three different templates were identified in which the zinc, the hydrophobic groups, the amido carbonyl, and the C-terminal carboxylic acid group of each inhibitor are superimposed onto the equivalent groups of the other inhibitors. All of the templates are in agreement in the conformation between the P₁' carbonyl and the terminal carboxylic acid regions of the inhibitors. However, they suggest different possible orientations between the zinc and the P₁' carbonyl. In template 1 and 2 compounds **12**, **13**, and benazeprilat, **14**, have essentially the same conformation as in template 1. However, the dihedral angles X and Φ of captopril, **11**, are in another low-energy conformation. Table 2 gives the dihedral angles defining the conformations captopril and benazeprilat adopt in the three templates.

The dihedral angles X and Φ of benazeprilat in template 1 were similar to the corresponding dihedral angles found in the X-ray structures of the first three inhibitors given in Table 1. When benazeprilat from superimposition 1 was superimposed on the composite X-ray data, a close match was found in the regions between the zinc and the P₁' side chain. Therefore, template 1 was selected as a pharmacophore for ACE. The four inhibitors in the conformation they adopt in template 1 are shown in Figure 4A (both individually and superimposed). The superimposition of benazeprilat from this template onto the X-ray structures is given in Figure 4B.

This template was subsequently used to analyze potential ACE/NEP inhibitors. The computer program TFIT⁶⁷ was used

(57) Patchett, A. A.; Cordes, E. H. In *Adv. Enzymol.*; Meister, A., Ed.; John Wiley & Sons: New York, NY, 1985; Vol. 57.

(58) Hangauer, D. G.; Monzinger, A. F.; Matthews, B. W. *Biochemistry* **1984**, *23*, 5730–5741.

(59) Watthey, J. W. H.; Gavin, T.; Desai, M. *J. Med. Chem.* **1984**, *27*, 816–818.

(60) Stanton, J. L.; Gruenfeld, N.; Babiars, J. E.; Ackerman, M. H.; Friedmann, R. C.; Yuan, A. M.; Macchia, W. *J. Med. Chem.* **1983**, *26*, 1267–1277.

(61) Ksander, G.; Bohacek, R. S.; de Jesus, R.; Yuan, A.; Sakane, Y.; Berry, C.; Ghai, R.; Trapani, A. J. Unpublished results.

(62) Mohamadi, F.; Richards, N. G. J.; Guida, W. C.; Liskamp, R.; Lipton, M.; G., C.; Chang, G.; Hendrickson, T.; Still, W. C. *J. Comput. Chem.* **1990**, *11*, 440–467.

(63) Fujinaga, M.; James, M. N. G. *Acta Crystallogr.* **1980**, *B36*, 3196–3199.

(64) Clarke, F. H. Personal communication.

(65) Hausin, R. J.; Codding, P. W. *J. Med. Chem.* **1990**, *33*, 1940–1947.

(66) McMartin, C.; Bohacek, R. Manuscript in preparation.

(67) McMartin, C.; Bohacek, R. *J. Comput.-Aided Mol. Design* **1995**, *9*, 237–250.

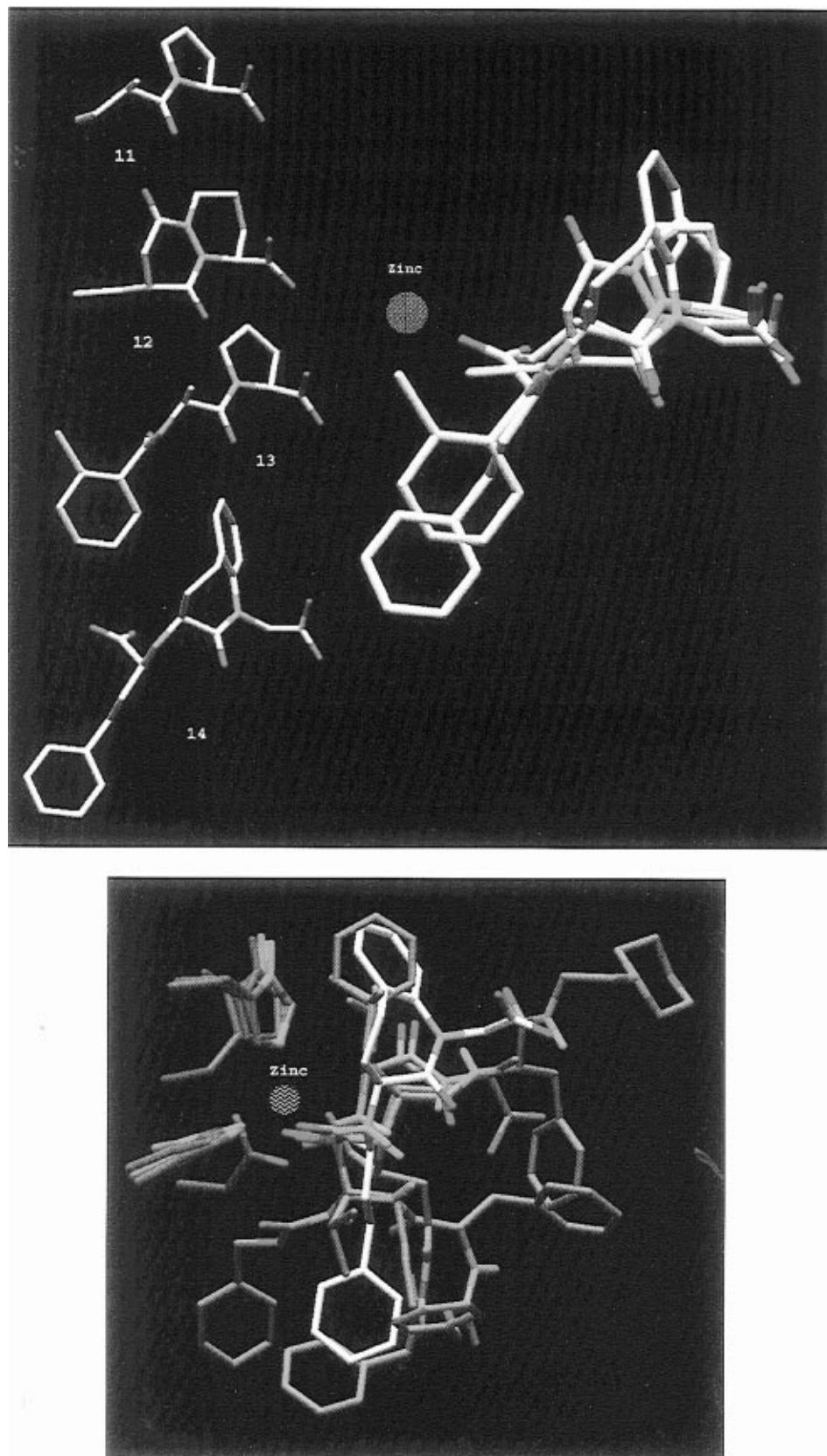


Figure 4. (A) (top) On the left, the ACE inhibitors, **11**–**14**, shown in Figure 3 in the conformation each inhibitor adopts to form the ACE inhibitor template. On the right, result of flexible superimposition of low-energy conformations of the ACE inhibitors superimposed so that the zinc, hydrophobic moieties, carbonyl oxygen, and terminal carboxylic acid of each inhibitor occupy the same relative positions. (B) (bottom) Benazeprilat in the conformation obtained by the flexible superimposition of the four ACE inhibitors shown in part A, superimposed onto the X-crystal structure of thermolysin complexed with ZFP(4) (**4**), carboxypeptidase A complexed with ZFVP(O)F (**5**), collagenase complexed with **3** and matrilysin complexed with **8** (also shown in Figure 1). The carbon atoms of benazeprilat are shown in white; those of the other inhibitors in brown and those of the enzymes are shown in gray.

to flexibly match molecules to the template using a superimposition force field. The output of the TFIT program is the

test structure superimposed on the template. Two parameters are also reported: the ligand strain energy which approximates

the cost in energy required for a test compound to adopt the superimposed conformation and the superimposition energy which is a measure of how closely atoms of the test compound can fit onto chemically similar atoms of the template. (See Experimental Section for more details.)

Model for NEP. The three-dimensional structure of NEP has also not as yet been reported. However, in this case, another related zinc metalloprotease, thermolysin, for which a number of high resolution crystal structures are readily available, has been used successfully as a model for NEP in the design of NEP inhibitors. Recent examples include the macrocyclic thiol **15**,⁶⁸ shown in Figure 5, and candoxatrilat,^{69,70} an analog of **2**.

There are striking similarities between the type of molecules which bind to NEP and to thermolysin. Both enzymes display similar substrate specificity and catalyze the hydrolysis of an amide bond on the amino side of hydrophobic residues. The type of compounds which inhibit these enzymes is also similar. For instance, both enzymes are strongly inhibited by the natural product phosphoramidon.^{71,72}

Some of the important similarities between NEP and thermolysin include the stereochemical requirements of the P₁' residue. Unlike ACE, both NEP and thermolysin are inhibited by (*S*)- and (*R*)-thiorphan (**6**), (*R*)-retro-thiorphan (**7**), and, to a lesser degree, by (*S*)-retro-thiorphan.^{53,73} This indicates that the volume around the base of the S₁' subsite must be similar in both enzymes. The position of the enzyme atoms which form hydrogen bonds to the amide group linking P₁' to P₂' are also likely to be very similar in the two enzymes as inferred from the ability of thiorphan, retro-thiorphan, and 10-membered ring lactams such as **15** to inhibit both NEP and thermolysin. Site-directed mutagenesis has been used to identify Arg¹⁰² as the residue in NEP which interacts with the C-terminal carboxylate of substrates and inhibitors binding to the S₁' and S₂' subsites.⁷⁴ The large increase in the K_i of retro-thiorphan (**6**) when binding to the Glu¹⁰² mutant compared to small changes in K_i for the retro-thiorphan analog where the C-terminal carboxylic acid had been replaced by amine strongly suggests that, similar to thermolysin, these inhibitors bind to the S₁' and S₂' subsites of NEP.⁷⁵ The relative orientations of the S₁' and S₂' subsites are also similar in the two enzymes. In thermolysin these pockets are connected. The crystal structures of several 10-membered macrocycles, including **15**, complexed to thermolysin have been determined and show that these molecules bind to the S₁' and S₂' subsites of thermolysin.⁷⁶ Since **15** is a very potent NEP inhibitor,⁶⁸ it can be hypothesized that this macrocycle also binds to the S₁' and S₂' pockets of NEP and that, as in thermolysin, these subsites form one contiguous accessible volume.

One of the significant differences between thermolysin and NEP is the size of the S₁' pocket. Inhibitors with a large group

such as a biphenylmethyl in P₁' are potent inhibitors of NEP but do not inhibit thermolysin.⁷⁷ Therefore, when using thermolysin as a model for NEP, it is important to know which are the areas inferred to be structurally similar to NEP and which parts appear to be significantly different.

In this work, the binding of a potential inhibitor to thermolysin/NEP was estimated using the MCDOCK module of the QXP molecular modeling program.⁶⁶ The molecule was docked into the thermolysin active site where different conformations and binding modes were explored and then energy minimized. The output of this program is an ensemble of low-energy conformations. For each conformation a total energy is reported as well as the ligand strain energy. The total energy (described in the Experimental Section) is useful as a qualitative parameter which, although it cannot predict binding affinities, does differentiate between those inhibitors which can form good interactions with an enzyme binding site and those that cannot. The strain energy is the difference in energy between the bound conformation of the ligand and the lowest energy conformation found after an exhaustive conformational search performed in the absence of the binding site. A ligand strain energy above 25 kJ is taken to be excessively high indicating that the bound conformation is not energetically accessible to that molecule.

The final evaluation of a docked structure is visual. After conformational searching and energy minimization in the binding site, the structures are scrutinized to determine if they can form the hydrogen bonds and hydrophobic interactions found in the crystal structures of numerous thermolysin/inhibitor complexes.⁷⁸

Dual Inhibitor Design Strategy. Our design strategy is outlined in Figure 5.

Thiorphan (**6**) is a potent inhibitor of NEP^{53,79} and a somewhat less potent inhibitor of thermolysin.^{73,80} The crystal structure of the thermolysin/thiorphan complex has been solved⁵¹ revealing that the benzyl substituent of thiorphan fills the S₁' subsite, while the amide forms hydrogen bonds with Arg²⁰³ and Asn¹¹², and the C-terminal carboxylic acid forms a hydrogen bond with Asn¹¹².

Thiorphan is also a modest inhibitor of ACE.⁵³ A low-energy conformation was found which allowed most of the atoms to superimpose onto the corresponding template atoms. However, the region occupied by the top of the phenyl ring is not defined by the template. In the discussion section, it will be shown that there are other potent ACE inhibitors with a phenyl group occupying a position close to that of the phenyl of thiorphan.

Thiorphan is a flexible molecule, allowing the carbonyl oxygen and the carboxylic acid group to adopt the conformation necessary to bind to NEP or ACE. However, it is likely that the loss of conformational restriction about the carboxylic acid contributes to the relatively weak binding to ACE. When the position of the carboxylic acid is fixed in a position ideal for binding to ACE resulting from the replacement of the glycine in thiorphan by a proline, the IC₅₀ in ACE drops from 0.13 μM (thiorphan) to 0.06 μM (proline analog). However, the proline analog places the terminal carboxylic acid in a position not

(68) MacPherson, L. J.; Bayburt, E. K.; Capparelli, M. P.; Bohacek, R. S.; Clarke, F. H.; Ghai, R. D.; Sakane, Y.; Berry, C. J.; Peppard, J. V.; Trapani, A. J. *J. Med. Chem.* **1993**, *36*, 3821–3828.

(69) Danilewicz, J. C.; Barclay, P. L.; Barnish, I. T.; Brown, D.; Campbell, S. F.; James, K.; Samuels, G. M. R.; Terrett, N. K.; Wythes, M. J. *Biochem. Biophys. Res. Commun.* **1989**, *164*, 58–65.

(70) Holland, D. R.; Karclay, P. L.; Danilewicz, J. C.; Matthews, B. W.; James, K. *Biochemistry* **1994**, *33*, 51–60.

(71) Komiyama, T.; Suda, H.; Aoyagi, T.; Takeuchi, T.; Umezawa, H.; Fujimoto, K.; Umezawa, S. *Arch. Biochem. Biophys.* **1975**, *171*, 727–731.

(72) Suda, H.; Aoyagi, T.; Takeuchi, T.; Umezawa, H. *J. Antibiot.* **1973**, *26*, 621–623.

(73) Benchetrit, T.; Fournié-Zaluski, M. C.; Roques, B. P. *Biochem. Biophys. Res. Commun.* **1987**, *147*, 1034–1040.

(74) Bateman, R. C., Jr.; Jackson, D.; Slaughter, C. A.; Unnithan, S.; Chai, Y. G.; Moomaw, C.; Hersh, L. B. *J. Biol. Chem.* **1989**, *264*, 6151–6157.

(75) Beaumont, A.; Barbe, B.; LeMoual, H.; Boileau, G.; Crine, P.; Fournié-Zaluski, M.-C.; Roques, B. P. *J. Biol. Chem.* **1992**, *267*, 2138–2141.

(76) Bohacek, R. S.; Priestle, J.; Grutter, M. Unpublished results, manuscript in preparation.

(77) De Lombaert, S.; Erion, M. D.; Tan, J.; Blanchard, L.; El-Chehabi, L.; Ghai, R.; Sakane, Y.; Berry, C.; Trapani, A. J. *J. Med. Chem.* **1994**, *37*, 498–511.

(78) Matthews, B. W. *Acc. Chem. Res.* **1988**, *21*, 333–340.

(79) NEP activity was measured using the synthetic substrate glutaryl-Ala-Ala-Phe-2-naphthylamide using the procedure described by Orlowski, M.; Wilk, S. *Biochemistry* **1981**, *20*, 4924–4950.

(80) Thermolysin activity was measured using the synthetic substrate glutaryl-Ala-Ala-Phe-2-naphthylamide using the procedure described by Pozsgay, M.; Michaud, C.; Liebman, M.; Orlowski, M. *Biochemistry* **1986**, *25*, 1292–1299.

	ACE IC ₅₀ (nM)	Structure	Match to ACE template. Superimposition energy, kJ. Strain energy, kJ. Description.	NEP IC ₅₀ (nM)	Structure	Docking into TLN model. Total Energy, kJ. Strain Energy, kJ. Description.
6	800		-219 4 Excellent match of backbone. No template for phenyl.	6		-26.1 3 Conformation found in X-ray structure of thiorphan bound to TLN.
15	29,700		--- 57 Superimposition of macrocycle on template highly strained. Hydroxy proline does not fit.	1		-31.6 4 Conformation verified by X-ray structure of this inhibitor bound to TLN.
14	6		---- 7 Part of template.	inactive		No low energy conformation found.
16	4.5		-429 7 Excellent match.	2.7		-31.4 10 Conformation similar to X-ray of thiorphan/TLN and 15/TLN. Almost identical to 18/TLN x-ray structure.
original ACE template	9.8					
18 CGS 28106	2		-439 10 Excellent match. (See Figure 6).	48		-31.7 7 Similar to 16/TLN model. Subsequently confirmed by X-ray of this inhibitor bound to TLN.

Figure 5. Cartoon outlining the strategy used for the design of a dual ACE/NEP inhibitor with suitable potency and pharmacokinetic profile. Thiorphan (**6**) is the prototype of a potent inhibitor of NEP but displays only moderate ACE inhibition. The potent macrocyclic NEP inhibitor **15** contains an additional α -amino acid residue which increases the distance between the terminal carboxylic acid and the internal amide. Such a relative spatial arrangement is poorly tolerated in ACE. The structural combination of thiorphan (**6**) and benzaprilat (**14**), a selective ACE inhibitor, leads to the β -thiol **16**, which possesses the functional groups required for tight binding to each enzyme and is flexible enough to allow these groups to occupy the position optimum for each enzyme. To further improve the potency of **16**, a fused proline residue was incorporated into the C-terminal portion of the molecule as suggested by the original template. Since β -thiols such as **16** often display poor pharmacokinetic properties, we envisioned that α -thiols with their increased steric hindrance around the sulfur, could display improved metabolic stability. Therefore, the thiol was moved from the β - to the α -position leading to compound **18**.

optimal for binding to NEP. While thiorphan inhibits NEP with a K_i of 0.002 μM , the proline analog has an IC_{50} of only 22 μM .⁸¹

Another potent NEP inhibitor is the macrocyclic compound, **15**,⁶⁸ which mimics a tripeptide. The crystal structure of the thermolysin/**15** complex has recently been determined showing that this macrocycle can bind to thermolysin in one of two different binding modes.⁷⁶ In one binding mode, similar to that of thiorphan, the macrocyclic portion occupies the S_1' and S_2' subsites, and the amide forms hydrogen bonds with Arg^{203} and Asn^{112} . However, **15** has an additional hydroxy proline residue in the S_3' subsite, and, therefore, the C-terminal carboxylic acid adopts a position different from that of thiorphan: it has shifted to the solvent side of Asn^{112} . Using thermolysin as a model, we hypothesized that thiorphan and the macrocyclic compound **15** bind to NEP in the same way, with the terminal carboxylic acid group of the macrocycle shifted to occupy the S_3' subsite.

Since both **15** and thiorphan are potent inhibitors of NEP, we conclude that **both** positions of the carboxylic acid are allowed for tight binding to NEP.

Not surprising, the macrocycle **15** is a poor ACE inhibitor.⁸² When superimposed onto the inhibitor template, no conformation could be found which would simultaneously superimpose the hydrophobic parts of the macrocycle, the carbonyl oxygen, and the carboxylic acid onto the corresponding atoms of the template. Superimposition of only the macrocycle onto the P_1' and P_2' portions of the template required significant distortion of the molecule shown by the excessive strain energy. (See Figure 5.)

The importance of the orientation of the carbonyl oxygen for optimal binding to ACE and NEP can be illustrated by the variation in activity of thiol macrocycles with different ring sizes. Although 10-membered macrocycles, like **15**, inhibit NEP, they are too constrained to allow the carbonyl to adopt

(81) Weller, H. N.; Gordon, E. M.; Rom, M. B.; Plusces, J. *Biochem. Biophys. Res. Commun.* **1984**, *125*, 82–89.

(82) ACE activity was measured using the substrate Hippuryl-His-Leu using the procedure described by Cushman, D. W.; Cheung, H. W. *Biochem. Pharmacol.* **1971**, *20*, 1637–1648.

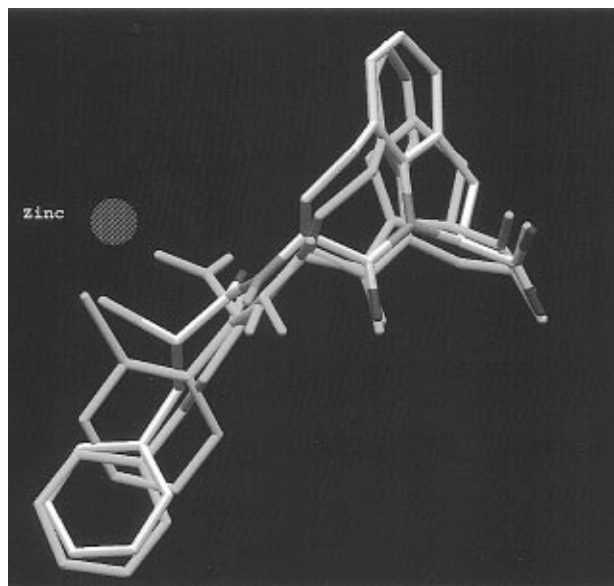


Figure 6. Compound **18** superimposed onto ACE inhibitor template. For clarity, only two of the inhibitors from the template are shown in yellow: **13** and benazeprilat (**14**).

the position necessary for hydrogen bonding to ACE. However, larger 13- and 14-membered macrocycles (lacking the hydroxy proline residue of **15**) inhibit both ACE and NEP. Modeling these macrocycles in our NEP and ACE models showed that these larger macrocycles are more flexible and allow the carbonyl oxygen to adopt the positions required by both enzymes.^{15,61}

The fact that both thiorphan and macrocycle **15** are potent inhibitors of NEP suggests that in NEP the C-terminal carboxylic acid can bind in the S_2' or the S_3' subsite. The large difference in activity of these two compounds in ACE suggests that, for strong binding to ACE, the C-terminal carboxylic acid group should occupy the S_2' subsite preferably fixed at the angle found in captopril. Therefore, to design a molecule which places the carboxylic acid in a position suitable for ACE and tolerated by NEP, the connection between the carboxylic acid portion of the molecule and the zinc binding portion must be sufficiently flexible to allow binding of the carboxylic acid group in the orientation required by **each** enzyme.

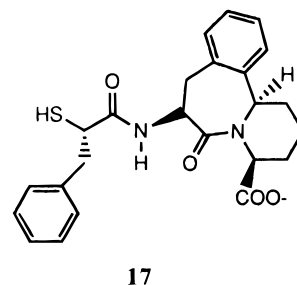
Potent ACE inhibitors such as benazeprilat (**14**)⁵⁵ are known in which the number of bonds separating the zinc and the terminal carboxylic acid are similar to that of the macrocycle **15**. However, **14** does not inhibit NEP to any significant degree. When modeled in the thermolysin model, no low-energy conformations could be found which would allow **14** to form the favorable interactions with the enzyme atoms found in the thermolysin/inhibitor crystal structures.

Compound **16** replaces the glycine of thiorphan with the bicyclic lactam portion of benazeprilat. When docked into the thermolysin active site, **16** occupies the S_1' , S_2' , and S_3' subsites. This molecule forms good interactions with the enzyme: similarly to thiorphan the amide bond forms hydrogen bonds with Arg²⁰³ and Asn¹¹². The penultimate carbonyl oxygen of compound **16** is in hydrogen bonding distance of Asn¹¹² and occupies the same position as one of the carboxylate oxygens of thiorphan. The terminal carboxylic acid of **16** is on the solvent side of Asn¹¹². Compound **16** also superimposes very well onto the ACE template. The phenyl group superimposes onto the P_1 phenyl of benazeprilat, the amide overlaps the amide of inhibitor **13** and the P_1' and P_2' portions of the molecule superimpose onto the corresponding parts of the template.

When synthesized, it proved to be a potent dual inhibitor of both ACE and NEP.

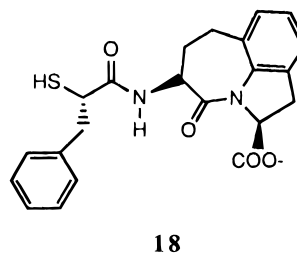
To further improve the potency of **16**, the conformation of the terminal carboxylic acid group was conformationally constrained into a position favorable for binding to ACE by the incorporation of a proline residue as suggested by the original ACE template. Since, β -thiols, such as **16**, usually display poor pharmacokinetic properties, we also wanted to improve this aspect of the compound.

One approach for improving the *in vivo* stability of such compounds is to decrease the chemical reactivity of the sulfur. Therefore, the steric hindrance around the sulfur was increased by moving the thiol from the β to the α position. α -Thiols have been shown to inhibit ACE⁵⁶ and other zinc metalloproteases.⁸³ More recently, Flynn et al.¹⁷ followed a similar strategy with the disclosure of **17** (MDL 100,173), a potent dual ACE/NEP inhibitor (ACE $K_i = 0.11$ nM; NEP $K_i = 0.08$ nM) containing an α -thiol functionality. Low-energy conformations



of **17** were identified which superimposed readily onto our ACE template. When docked into the thermolysin model, a low-energy conformation was found in which the inhibitor occupied the S_1' , S_2' , and S_3' subsites forming the same interactions with the enzyme as compound **16** and similar to those found in the X-ray structures of thermolysin/inhibitor complexes. (Also see Table 4.)

Incorporating the proline ring and the α -thiol functional group led to the tricyclic α -thiol **18** (CGS 28106). This structure



superimposed extremely well onto the ACE template (Figure 6). The phenyl was superimposed onto the P_1 phenyl of benazeprilat, the amide overlapped the amide of **13**, the P_1' and P_2' portions overlapped the corresponding atoms of the template, and the conformationally constrained carboxylic acid was superimposed on the C-terminal carboxylic acids of the template. When subjected to energy minimization in the active site of thermolysin, this compound formed the same favorable interactions with the enzyme as found in the thermolysin/thiorphan and thermolysin/**15** crystal structures. The phenyl ring occupied the S_1' subsite, the amide formed hydrogen bonds with Arg²⁰³ and Asn¹¹², the penultimate carbonyl made a hydrogen bond with Asn¹¹², and the carboxylic acid group occupied a position to the solvent side of Asn¹¹². Thiol **18** was readily synthesized by acylation of the tricyclic amino ester core⁸⁴ followed by saponification (see supporting information) and found to be a potent inhibitor of both ACE ($IC_{50} = 40$ nM) and NEP ($IC_{50} =$

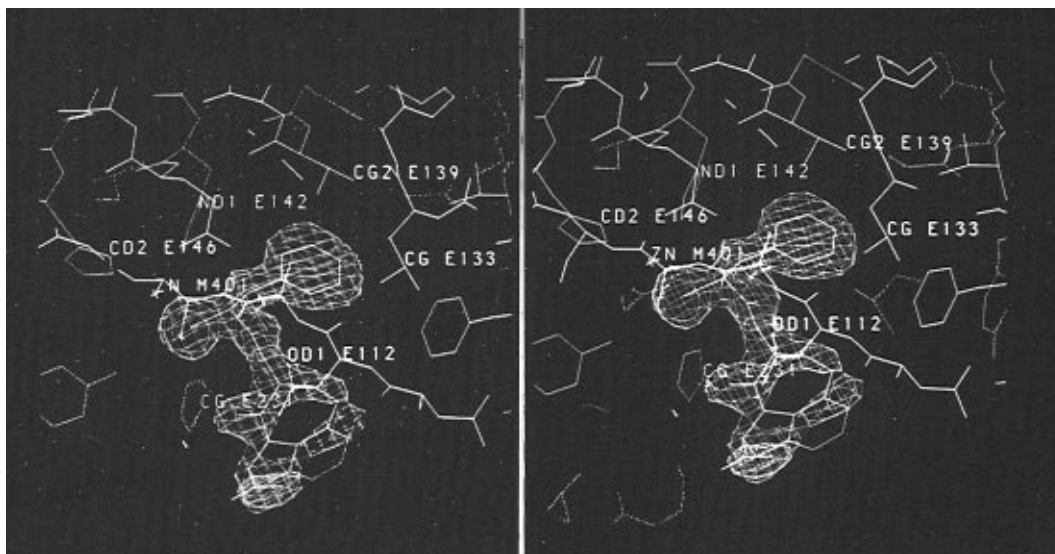


Figure 7. Stereo picture of the $F_o - F_c$ electron density (contoured at three standard deviations above the mean) at 1.9 Å resolution showing the inhibitor **18** bound to thermolysin. The inhibitor is shown in green. The electron density around the sulfur, phenyl group, and amide group is very clear, indicating tight binding. However, it is less clear around the tricyclic moiety which extends into the solvent.

48 nM) and, to a smaller degree, of thermolysin ($IC_{50} = 1.6 \mu M$).

The biological activity of compound **17** was also determined under the same conditions as those used for **18** resulting with an IC_{50} for **17** of 30 nM in ACE and 14 nM in NEP. Similar activities for **17** in ACE ($IC_{50} = 32$ nM) and NEP ($IC_{50} = 9$ nM) were reported by Robl et al.⁹³

X-ray Crystallography. In the absence of structural data, there has been considerable speculation about how α -thiols bind to zinc metalloproteases. A bidentate mode, with the sulfur and the adjacent carbonyl oxygen binding to zinc, has been proposed.⁸⁵ When modeling the tricyclic thiol **18** in the active site of thermolysin, we found that this molecule could form favorable interactions with the enzyme provided that the sulfur interacts with the zinc in a monodentate fashion analogous to thiorphan. Thus, even though **18** has one less carbon atom between the sulfur and the carbonyl than thiorphan, the phenyl and amide groups could be modeled to fit into the active site in a manner very similar to thiorphan. However, the difference between α - and β -thiols is large enough that it was decided to determine experimentally how **18** actually binds to thermolysin. Therefore, the three-dimensional structure of this inhibitor bound to thermolysin was determined using X-ray crystallography (see Experimental Section).

Figure 7 shows the electron density map of the tricyclic α -thiol **18** bound to thermolysin. The sulfur binds in a monodentate fashion. The distance between the sulfur and zinc is 2.3 Å, the same distance as was found in the crystal structure of thermolysin inhibited with the β -thiol thiorphan.⁵¹ The position of the sulfur atom is practically identical in the two complexes, but, even more interestingly, the positions of the α -carbons are also very similar. The difference is in the C–S–Zn bond angle, which is rather distorted in the thiorphan complex (122 degrees), while in the complex with **18** this angle is closer to the value (99 degrees) found in crystal structures of small molecules.⁶⁵

The phenyl ring is located in the hydrophobic S_1' subsite and the carbonyl and NH groups of the amide form hydrogen bonds

(83) Van Amsterdam, J. G. C.; Van Buuren, K. J. H.; Blad, M. W. M.; Soudijn, W. *Eur. J. Pharmacol.* **1987**, *135*, 411–418.

(84) De Lombaert, S.; Blanchard, L.; Stamford, L. B.; Sperbeck, D. M.; Grim, M. D.; Jenson, T. M.; Rodriguez, H. R. *Tetrahedron Lett.* **1994**, *35*, 7513–7516.

(85) Holmquist, R.; Vallee, B. L. *Proc. Natl. Acad. Sci. U.S.A.* **1979**, *76*, 6216–6220.

with the side chains of Arg 203 and Asn 122, respectively. Most of the tricyclic moiety extends out toward the solvent. The poor electron density of the tricyclic moiety indicates that its position is not well defined in the complex with thermolysin, implying only tenuous interactions with the enzyme. Examination of the refined isotropic temperature factors (B-factors) of the individual atoms of the inhibitor bears this out. Whereas the B-factors of the sulfur atom, phenyl group, and amide group (15–20 Å²) are on the same order as that for the zinc atom, implying little movement and tight binding, those for the tricyclic moiety increase to between 30–50 Å².

Figure 8 is a stereo image which shows a comparison between the bound conformation of **18** as determined by X-ray crystallography and predicted by molecular modeling. The excellent agreement supports our working hypothesis.

Discussion

We have described the design strategy leading to the discovery of a potent dual ACE and NEP inhibitor and proposed the conformations such molecules adopt when they bind to both of these enzymes. However, without direct experimental evidence such as the X-ray crystal structure of the enzyme/inhibitor complex or transfer NOE experiments which can determine the bioactive conformation,⁸⁶ it is impossible to be completely certain about the binding modes of ACE/NEP inhibitors. The credibility of computationally derived templates can be enhanced by considerations of the mechanism of action and comparisons with the available structural data, as described above. Comparisons with templates constructed by other researchers and rigorous testing of our models to see if they can distinguish between the active and inactive compounds reported by other groups are additional ways to further evaluate the three-dimensional models and hypothesis proposed in this work and are described in the next section.

Comparison to Previously Reported Models of ACE. A variety of methods have been previously used to predict the bioactive conformations of ACE inhibitors. Three research groups have used conformational analysis to identify all the low-energy conformations of the inhibitors studied in order to identify a common, low-energy conformation available to all

(86) Gonnella, N.; Bohacek, R. S.; Zhang, X.; Kolossvary, I.; Paris, C. G.; Melton, R.; Winter, C.; Hu, S.; Ganu, V. *Proc. Natl. Acad. Sci. U.S.A.* **1995**, *92*, 462–466.

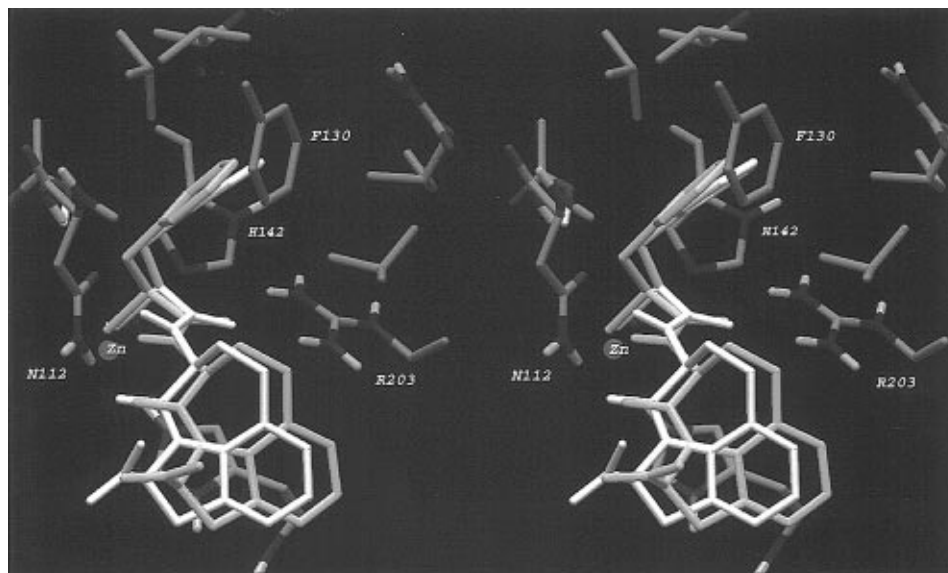


Figure 8. A stereo picture of the dual inhibitor **18** bound to thermolysin. In white is the conformation predicted by molecular modeling and in green is the conformation subsequently determined by X-ray crystallography. Relevant atoms of the thermolysin binding site are shown in darker colors.

the molecules in the series.^{87–90} More recently, a fourth group suggested that the conformation adopted by four ACE inhibitors in the solid state as determined by X-ray crystallography could also be the bioactive conformation in ACE.⁶⁵

One of the first three-dimensional models of the bioactive conformation of ACE inhibitors was developed by Hassall et al.⁸⁷ By identifying the positions that the sulfur, carbonyl, and carboxylic acid atoms adopt in the low-energy conformations of captopril, Hassall et al. developed a three-dimensional model⁸⁷ which they used to design rigid bicyclic inhibitors.⁸⁸ Molecule **12** in Figure 2, one of the inhibitors used to construct our template, is the most potent compound from this series. Hassall et al. present their results as a mesh indicating positions energetically accessible to each of the inhibitors atoms studied. In agreement with our results, their mesh plot indicated two allowed positions for the sulfurs: one with a Φ near 168° and another (although it is difficult to tell from their plot) near -60° . The latter is similar to our template.

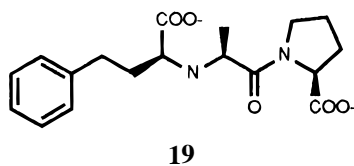
A thorough conformational analysis of eight ACE inhibitors was reported by Andrews et al.⁸⁹ They used this analysis to identify a low-energy conformation common to all the inhibitors of the series. Energies were calculated using fixed bond lengths and bond angles and disregarding electrostatics interactions. This is significantly different from the methods used in this study. The TFIND program used in our analysis performs a full Cartesian minimization using all the terms of a potential energy function. The conformational energy contour map computed by Andrews et al. for Φ vs Ψ of captopril revealed results qualitatively similar to those obtained with our methods: two “global” minima, one at $\Phi \sim 180^\circ$, $\Psi \sim 120^\circ$ and another at $\Phi \sim -60^\circ$, $\Psi \sim 180^\circ$. In agreement with our results, Andrews et al. selected the conformation with $\Phi \sim -60^\circ$.

Andrews et al. constructed the remaining portions of their ACE inhibitor model by computing contour energy maps of the torsion bonds defining the P_1 and P_2 portions of enalaprilat

(**19**), ketoace (**21**), and two analogs with phosphonic acid zinc binding groups. They then identified low-energy conformers that could be superimposed onto the thiols. The exact values of the angles used were not given. Instead stereo plots of the bioactive conformation predicted for each molecule were presented. We reconstructed the model of Andrews et al. by constructing the inhibitors to match their pictures and *rigidly* superimposing these structures. The result gave close overlap of the atoms of the P_1' and P_2' regions. However, in our hands, the P_1 portions could not be superimposed. Our template was constructed using a superimposition force field to *flexibly* fit the molecules. This results in small changes of the torsion angles leading to a much better superposition of all parts of the molecules. The conformers, however, still maintain low internal energies as reported in Figure 5 and Table 4. We then used TFIT to flexibly fit the compounds used by Andrews et al. resulting in a close overlap of all parts of the inhibitors. This model is similar to template 1, that is, it agrees with our model for the orientation of the Φ and Ψ but has a different conformation for the binding to the zinc.

A different approach for constructing an ACE inhibitor template was undertaken in the laboratory of Marshall by Mayer et al.⁹⁰ In that study, the enzyme atoms from the ACE active site which were assumed to bind with the inhibitor atoms were added to each inhibitor. Thus, a zinc was added to the zinc binding group, an NH which formed a hydrogen bond was added to the amide carbonyl, and an arginine-guanidinium ion was positioned to form an electrostatic interaction with the terminal carboxylic acid. Low-energy conformations of 28 ACE inhibitors were then identified that possessed the proper relative orientations of the active site groups common to all ligands. The results of this study were presented in the form of distances between key atoms of the template.

To compare this template with ours, we constructed molecule **20** with the intermolecular distances given by Mayer et al. When

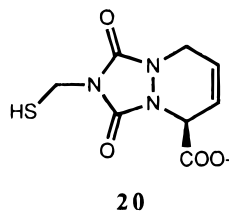


(87) Hassall, C. H.; Kroehn, A.; Moody, C. J.; Thomas, W. A. *FEBS Lett.* **1982**, *147*, 175–179.

(88) Hassall, C. H.; Kroehn, A.; Moody, C. J.; Thomas, W. A. *J. Chem. Soc., Perkin Trans. 1* **1984**, 155–164.

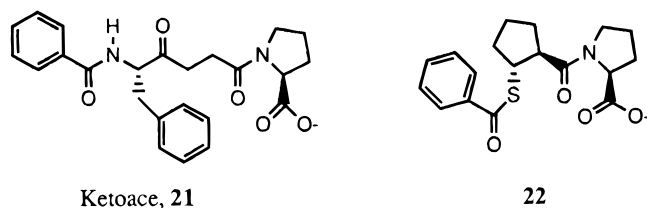
(89) Andrews, P. R.; Carson, J. M.; Caselli, A.; Spark, M. J.; Woods, R. *J. Med. Chem.* **1985**, *28*, 393–399.

(90) Mayer, D.; Naylor, C. B.; Motoc, I.; Marshall, G. R. *J. Comput.-Aided Mol. Des.* **1987**, *1*, 3–16.



this structure is superimposed onto our template, it becomes apparent that the P_1' and P_2' portions of the templates are similar but that regions between P_1' and the zinc are different. This structure has X (Zn-S-C-C angle) of 159° , ϕ of 98° , and Ψ of -176° . When **20** was fitted to our template with the TFIT program, the best fit had a X of -70 , Φ of -87 , and Ψ of 178° . Because not enough geometrical information is given in their paper about the orientation of the P_1 portions of ACE inhibitors, it is difficult to build their template with our computational tools. However, it appears that this template is significantly different from the templates we have constructed.

Another study of the biological conformation of ACE inhibitors was reported by Hausin and Coddling.⁶⁵ They determined the crystal structure of two ACE inhibitors, **21** and **22**. Using carefully selected parameters from X-ray crystal



structure data, they added a zinc to the crystal structure conformation of these two inhibitors as well as to the crystal structure of captopril and hippuryl-L-histidyl-L-leucine. They then found that by not defining the Zn-S-C-C bond, they were able to superimpose the crystal structure conformation of all four structures and suggested, based on energy calculations, that this could be the bioactive conformation of these inhibitors. However, we found that the *rigid* superimposition of the X-ray crystal structures conformers does not give a good match for the P_1 and P_2 portions of these molecules. When the rigid superimposition of the X-ray structures were subjected to the flexible superposition force field, a good match between all parts of the molecules was found, and the resulting conformations of the inhibitors was similar to template 3.

Coddling and Hausin left the Zn-S-C-C torsion angle undefined because of the large variety found for this angle in the X-ray structures of small molecules and the thermolysin/inhibitor complexes. However, by considering the likely mechanism of zinc-metallo proteases and the X-ray data described earlier, we believe that it is possible to deduce approximate values for this angle adopted by inhibitors when binding to ACE.

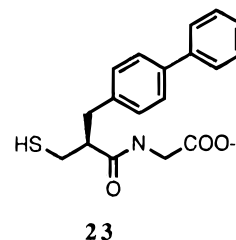
In conclusion, because potent ACE inhibitors have been designed in which the P_1' and P_2' portions are highly constrained, all of the ACE inhibitor templates are in agreement as to the bioactive conformation of the regions between the P_1' carbonyl and the terminal carboxylic acid. However, since previous researchers did not fully consider the X-ray data of zinc metalloproteases for the mechanism of action suggested by this data, their models differ from each other and from our model in the orientation that the inhibitors display relative to the catalytic zinc. In addition, the new flexible superimposition program, TFIND, represents a breakthrough in the computational methods available for superimposing structures which was not available to these researchers. Use of the TFIND program improved the models proposed by Andrews and Hausin

identifying common conformations of the P_1 and P_2 portions of the ACE inhibitors which they studied.

Evaluation of the NEP Model. The crystal structure of thermolysin has been useful as a model for NEP. Several novel, potent NEP inhibitors have been designed using the thermolysin active site as a model.^{68,69} The crystal structure of **18** bound to thermolysin is significant because it shows that an α -thiol can bind to a zinc atom in a monodentate manner thus allowing the entire molecule to bind to the S_1' , S_2' , and S_3' subsites of the enzyme. We propose that **18** binds to NEP in an analogous manner.

Scientists at the Université René Descartes and Rhône Poulenc Rorer have synthesized a series of NEP inhibitors of the type HS-CH(R_1)-CH₂-CH(R_2)-CONH-CH(R_3)-COOH to investigate the S_1 subsite of NEP.⁹¹ Using the NEP mutant in which Arg²⁰² has been changed to Glu²⁰², they concluded that these inhibitors do not bind to the S_1 subsite but rather that the R_1 and R_2 groups bind to the S_1' and S_2' subsites, respectively, and that the C-terminal residue is in solvent outside of the binding site. In agreement with our model, they concluded that thiol inhibitors are not well adapted for optimal recognition of the S_1 subsite of NEP.

With the discovery of the conformationally restricted NEP inhibitor **18** described in this work, it is now possible to construct a template for NEP inhibitors in a manner analogous to that used in this work for ACE. Three potent NEP inhibitors were used to construct the NEP template: **23** a biphenyl analog



of thiorphan (IC_{50} in NEP = $0.004 \mu M$), the macrocycle **15**, and the tricyclic dual inhibitor, **18**. Together these inhibitors provide information about the relatively deep S_1' subsite (likely binding site for the biphenyl moiety) and the orientation of the S_1' , S_2' , and S_3' subsites. Low-energy conformations of all three inhibitors were identified which allowed for superimposition of chemically similar atoms using the TFIT program. Table 3 gives the dihedral angles defining the various superimpositions found by the program. Superimposition 1 is shown in Figure 9. The conformation these three compounds adopt is very similar to the conformation thiorphan, **15**, and **18** adopt when bound to thermolysin as shown by the crystal structure of these inhibitors complexed with thermolysin. The agreement between these two models for NEP supports our original hypothesis.

To test the NEP inhibitor template, conformations were sought which would allow retro-thiorphan, an active NEP inhibitor, to be superimposed onto the template. A low-energy conformation was readily found. To test the template with an inactive compound, captopril was fitted onto the NEP template. No low-energy conformations of captopril were found which simultaneously allowed the superimposition of the zinc, methyl side chain, carbonyl, and carboxylic acid on the corresponding atoms of the NEP template.

Analysis of the Structure Activity Relationship of Other Dual ACE/NEP Inhibitors Using Our Models. Recently, other dual ACE/NEP inhibitors have been reported. We used the models proposed here to rationalize the structure activity relationships found in other laboratories and to compare our

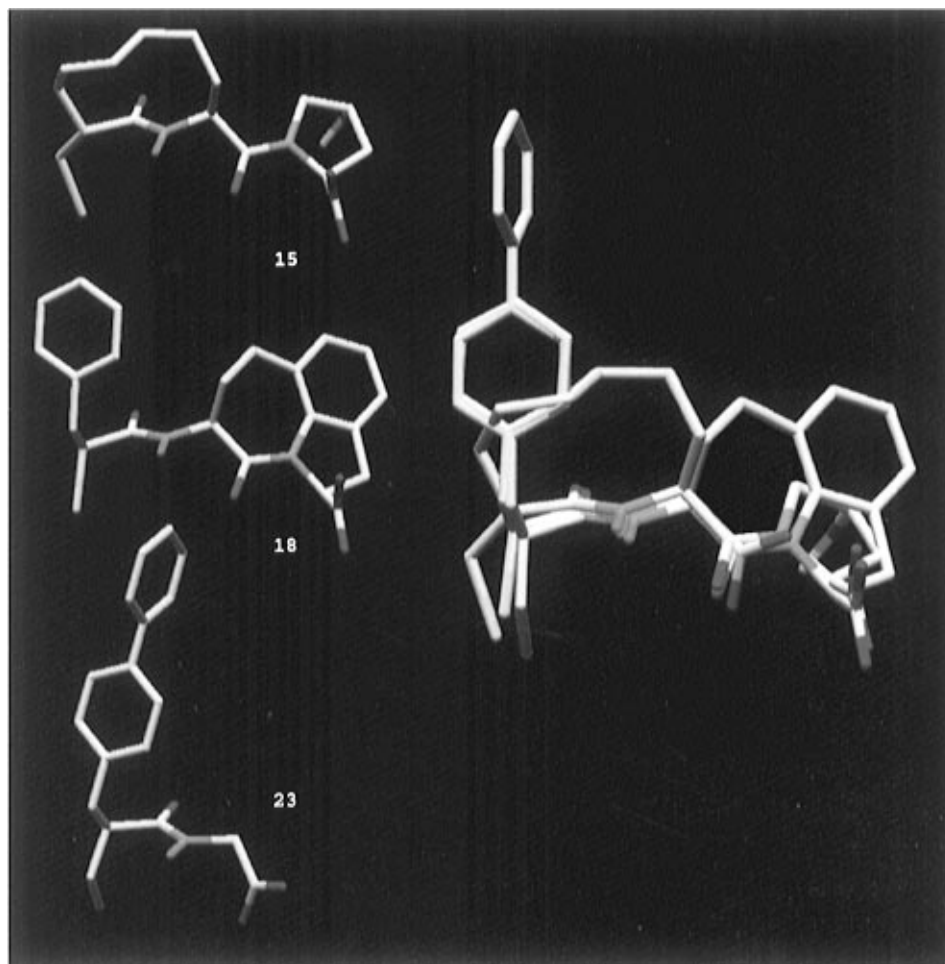


Figure 9. On the left, the NEP inhibitors **15**, **18**, and **23** in the conformation each inhibitor adopts to form the NEP template. On the right, result of flexible superimposition of low-energy conformations superimposed so that chemically similar atoms occupy the same relative positions producing a composite NEP inhibitor template.

Table 3. NEP Inhibitor Template. Characteristics of the Best Superimpositions Found by TFIT: Geometry of Thiorphan Analog, **23**, Volume of the Three Superimposed Inhibitors, and Strain Energies of Each Inhibitor

superimposition	dihedral X Zn-S-C-C	dihedral Φ	dihedral Ψ	vol. ^a (\AA^3)	strain energy ^b (kJ)		
					15	18	23
1 ^c	-72.8	-63.0	-68.5	452	4	4	2
2	86.1	-70.0	-73.7	451	2	6	4
3	-94.5	-169.6	-74.6	448	4	6	4
4	87.4	-166.6	-71.9	455	4	3	4
5 ^d	-71.0	-62.6	128.8	457	0	11	3

^a The total volume of the four superimposed inhibitors. ^b The difference in energy between the global minimum and the energy of the conformation in the superimposition. ^c Superimposition predicted to be the bioactive conformation. ^d Amide bond rotated $\sim 180^\circ$.

models to those proposed by other researchers. All the results are summarized on Table 4.

Using thiorphan as a starting point, Gros et al.¹⁹ designed two new dual ACE/NEP inhibitors, glycopril and alatriopril. Addition of a methylenedioxy ring to the phenyl of thiorphan resulted in glycopril and the substitution of alanine for the terminal glycine of thiorphan and glycopril gave alatriopril (**24**). (See Table 4.) They proposed that the phenyl methylenedioxy moiety binds to the S_1 subsite of ACE, as has been proposed for the phenyl of enalaprilat (**19**).²²

To examine their hypothesis, we first used the TFIT program to determine if there was a common conformation of **24** and

enalaprilat in which the phenyl rings, the carbonyl, and terminal carboxylic acid groups could be superimposed. None was found. Next, the TFIT program was used to determine what low-energy conformers of **24** matched our ACE template. Although the template does not have substituents which extend into the P_1' region and, hence, is not a good model for the phenyl methylenedioxy portion of **24**, a conformation in which **24** superimposed well on the remaining sections was found. However, the potent tricyclic ACE inhibitors **17** and **28** contain a conformationally restricted phenyl ring which, according to our model, binds to the S_1' subsite of ACE. The superimposition of these inhibitors onto the ACE template extends our knowledge of the space available for inhibitor atoms. Considerable overlap of the phenyl group of **24** with the template superimposed conformations of **17** and **28** was found. On the other hand, visual inspection and the superimposition energy showed that **25**, the less active *R*-isomer of **24**, did not fit onto the template quite as well. More significant, there was less overlap of the phenyl ring of **25** with the corresponding phenyl rings of our model of **17** and **28**. In conclusion, we predict in contrast to the model proposed by Gros et al., that **24** binds to ACE with the phenyl methylenedioxy group in the S_1' subsite.

Gros et al. proposed that the phenyl methylenedioxy group of their series binds to the S_1' pocket of NEP. We could not use our thermolysin model of NEP to model **24** and **25** since these compounds have a long side chain in the P_1' position and thermolysin is not a good model for the deeper S_1' pocket of NEP. Therefore, we used the NEP inhibitor template. Low-energy conformations were identified by TFIT in which the phenyl methylenedioxy group fit into the S_1' subsite as suggested

(91) Gomez-Monterrey, I.; Beaumont, A.; Nemecek, P.; Roques, B. P.; Fournié-Zaluski, M. C. *J. Med. Chem.* **1994**, *37*, 1865-1873.

Table 4. Evaluation of Dual ACE/NEP Inhibitors Using the ACE and NEP Models

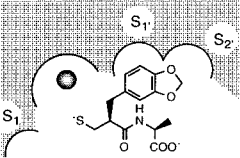
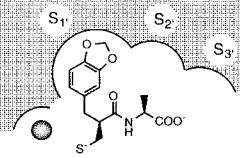
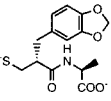
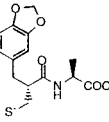
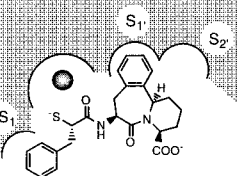
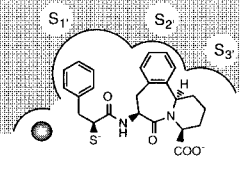
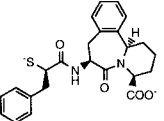
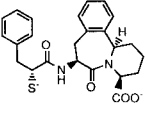
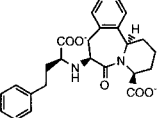
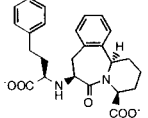
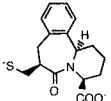
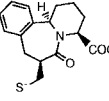
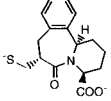
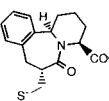
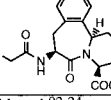
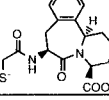
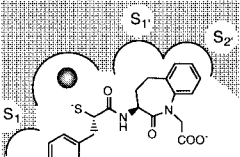
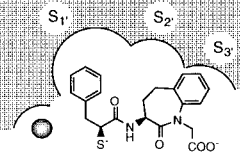
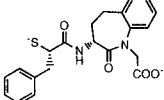
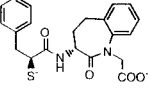
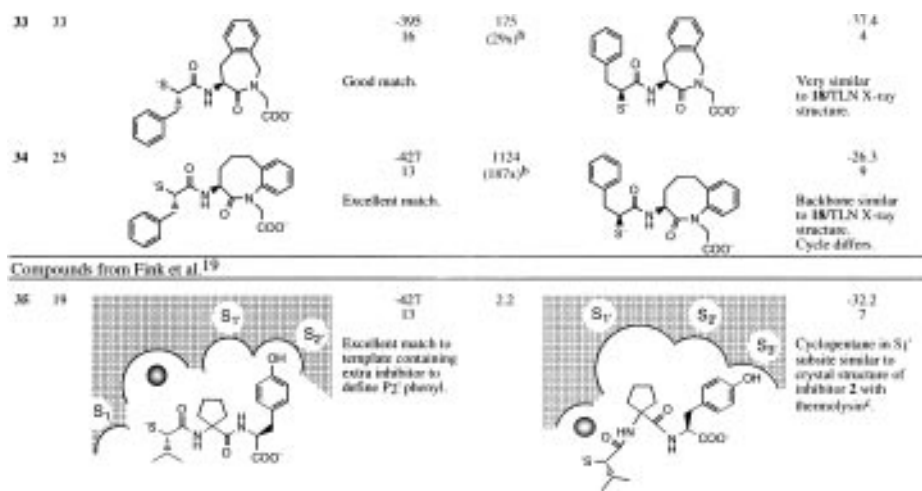
ACE IC ₅₀ (nM)	Proposed binding mode in ACE	Match to ACE template Superimposition energy, kJ Strain energy, kJ Description	NEP IC ₅₀ (nM)	Proposed binding mode in NEP	Match to NEP template Superimposition energy, kJ Strain energy, kJ Description	
Compounds from Gros et al.¹⁹						
24	9.8		-239 6	5.1		-290 6 Good match. Phenyl superimposes on phenyl of 23.
25	215		-237 6 Less satisfactory superimposition than 24. Little overlap with superimposition of 17 and 28.	13.7		-288 9 Methylene dioxy phenyl does not superimpose as well as 24.
ACE IC ₅₀ (nM)	Proposed binding mode in ACE	Match to ACE template Superimposition energy, kJ Strain energy, kJ Description	NEP IC ₅₀ (nM)	Proposed binding mode in NEP and TLN	Docking into thermolysin model Total energy, kJ Strain energy, kJ Description	
Compounds from Flynn et al.¹⁷						
17	0.11		-425 13 Excellent match.	0.08		-38.2 4 Almost identical to 18/TLN X-ray structure.
26	4.5		-421 16 Good match but P1 phenyl does not superimpose as well as 17.	0.07		-32.5 5 Slightly different from 18/TLN X-ray structure.
27	9.8		-436 13 Excellent match.	>10,000		95 49 No low energy conformation.
28	2		-316 2 Good match.	>300		10.8 9 Does not form favorable interactions with enzyme.
29	>7		-303 3 Good match.	45 (-x642) ^a		5.2 24 Does not form favorable interactions with enzyme.
30	2		-345 9 Excellent match.	5 (-x71) ^a		-15.2 6 Similar to 18/TLN X-ray structure. Does not fill S1' subsite.
Compounds from Robl et al.⁹²⁻²⁴						
31	12		-426 11 Excellent match.	6		-31.9 5 Almost identical to 18/TLN X-ray structure.
32	306		-431 46 Excellent match. Excessive strain energy.	560 (93x) ^b		-28.4 9 The cycle cannot adopt conformation like that of 18/TLN X-ray structure.

Table 4 (Continued)



^a Decrease in potency in comparison to **26**, the most potent NEP inhibitor in the series. ^b Decrease in potency in comparison to **31**, lead compound in series. ^c Structure 1THL in the Brookhaven Protein Data Bank.

by Gros et al. The superimposition of the *R*-isomer, **25**, was less satisfactory.

Flynn et al.¹⁷ discovered another series of dual ACE/NEP inhibitors (modeling of the most active compound from this series, **17**, has been described above in the section on Inhibitor Design). They proposed models for the bio-active conformation of these inhibitors based on two energetically allowed conformations of a hypothetical substrate. In agreement with our model, they propose that their inhibitors bind to ACE with the phenyl in the S₁' subsite of ACE. However, their hypothesis for how the inhibitors bind to NEP is significantly different from ours. They propose that the zinc is on the opposite side of the scissile bond from our model for NEP and the X-ray data. Since NEP and thermolysin are so similar in their specificities, we believe it is unlikely that NEP, in contrast to all of the structural X-ray data reported for zinc metalloproteases, reverses the positions of the catalytic site.

To further test our hypothesis, all the inhibitors reported by Flynn et al. were modeled with our models. The results are summarized in Table 4. The ACE inhibitor template used in this study is a good model for their compounds. TFIT found low-energy conformations of all of their ACE inhibitors which match the template well. The superimposition energy correlated with the differences in *K_i* of stereoisomers.

To determine if our thermolysin model can distinguish between the active and inactive NEP inhibitors reported by Flynn et al., we docked each compound into the active site of thermolysin using the protocol described in the experimental section. With a single exception, low-energy conformations were found for all the potent NEP inhibitors which formed good interactions with the binding site atoms and closely resembled the crystal structure of **18** bound to thermolysin. On the other hand, for the inactive compounds, no low-energy conformations were found which were able to form favorable enzyme interactions. The exception was compound **29**. Flynn et al. reported that this compound has a *K_i* of 45 nM in NEP. Although the interaction energy is somewhat more favorable than that of the less active compound **28**, the thermolysin model would predict that **29** does not bind well to NEP. Although, in their assays **29** is a potent NEP inhibitor, it must be pointed out that **29** is almost 650 times less potent than their best compound. It may also be that the P₁' pocket in NEP is not only longer but also somewhat wider, and, therefore, thermolysin is not a particularly good model for this region of NEP.

Another series of dual ACE/NEP inhibitors have been designed by Robl et al.⁹²⁻⁹⁴ They proposed a two-dimensional

model that is consistent with our three-dimensional models for both ACE and NEP. To further test our models, we explored the structural activity relationships reported by this group. A number of structurally diverse inhibitors from their series were selected and modeled in thermolysin and with our ACE inhibitor template. As shown in Table 4, low-energy conformations which matched the ACE template were found by the TFIT program for those compounds which were good ACE inhibitors. For the compound with poorer activity, superimposition on the template required significant distortion as indicated by the high strain energy.

The thermolysin model gave results which were reasonably consistent with the model. The relatively good compounds fit well into the thermolysin active site, formed interactions similar to those found in the crystal structure of **18** bound to thermolysin, and displayed favorable energies. Although poorer inhibitors positioned the P₁' phenyl ring nicely into the S₁' subsite of thermolysin, the macrocycles could not adopt conformations similar to those of the active compounds. The reduction in favorable contacts was reflected in the higher energies of these compounds.

A dual ACE/NEP inhibitor (**35**), structurally significantly different from those reported by other researchers, was developed by Fink et al. at Ciba.⁹⁵ Because this inhibitor has a tyrosine in the P₂' subsite, we added **2** to the ACE template. This inhibitor fits well onto the template. Our model predicts that the isopropyl group binds to S₁ subsite of ACE and the cyclopentyl group binds to the S₁' subsite. Modeling of this compound in thermolysin predicted that **35** binds with the isopropyl and cyclopentyl group in the S₁ and S₁' subsites, respectively. Our model predicts that this is the binding mode in which **35** binds to NEP.

(92) Robl, J. A.; Simpkins, L. M.; Sulsky, R.; Sieber-McMaster, E.; Stevenson, J.; Kelly, Y. F.; Sun, C.; Misra, R. J.; Ryono, D. E.; Asaad, M. M.; Bird, J. E.; Trippodo, N. C.; Karanewsky, D. C. *Bioorg. Med. Chem. Lett.* **1994**, *4*, 1795-1800.

(93) Robl, J. A.; Simpkins, L. M.; Stevenson, J.; Sun, C.; Murugesan, N.; Barrish, J. C.; Asaad, M. M.; Bird, J. E.; Schaeffer, T. R.; Trippodo, N. C.; Petrillo, E. W.; Karanewsky, D. C. *Bioorg. Med. Chem. Lett.* **1994**, *4*, 1789-1794.

(94) Delaney, N. G.; Barrish, J. C.; Neubeck, R.; Natarajan, S.; Cohen, M.; Rovnyak, G. C.; Huber, G.; Murugesan, N.; Girotra, R.; Sieber-McMaster, E.; Robl, J. A.; Asaad, M. M.; Cheung, H. S.; Bird, J. E.; Waldron, T.; Petrillo, E. W. *Bioorg. Med. Chem. Lett.* **1994**, *4*, 1783-1788.

(95) Fink, C. A.; Qiao, Y.; Berry, C. J.; Sakane, Y.; Ghai, R. D.; Trapani, A. J. *J. Med. Chem.* **1995**, *38*, 5023-5030.

Conclusions

To aid in the design of dual ACE/NEP inhibitors, a novel three-dimensional ACE inhibitor template has been constructed using a new computer program which flexibly matches molecules using a superposition force field. The conformation that this inhibitor template adopts in the region close to the zinc matches that found in the crystal structures of four different zinc metalloproteases complexed with potent inhibitors. Compounds known to inhibit ACE, including the new dual ACE/NEP inhibitors described here as well those reported by other groups, readily matched this template, whereas inactive compounds could not be superimposed. The crystallographically determined binding site of thermolysin was found to be a good model for most NEP inhibitors.

These three-dimensional models predict that α -thiol tripeptide mimics bind to the S_1 , S_1' , and S_2' subsites of ACE and in a different binding mode to the S_1' , S_2' , and S_3' subsites of NEP. The usefulness of these models has been demonstrated by providing an insight on the specific binding modes of **18** (CGS 28106), a potent dual ACE/NEP inhibitor currently under pharmacological investigation. These powerful tools should prove very valuable for the structure-based design of even more potent inhibitors.

The X-ray crystal structure of an α -thiol bound to a zinc metalloprotease has been reported for the first time. As predicted by modeling, the α -thiol, **18**, occupies the S_1' , S_2' , and S_3' subsites of thermolysin. The X-ray structure showed that the sulfur and α -carbon positions are very similar to those found in the structure of the β -thiol thiorphan bound to thermolysin. However, the Zn–S–C bond angles are significantly different. When compared to thiorphan, the C-terminal carboxylic acid group has shifted occupying the S_3' subsite on the solvent side of Asn¹¹². These findings support our hypothesis regarding how these types of inhibitors bind to NEP.

Based on these findings, an NEP inhibitor template was constructed which also discriminated between the active and inactive compounds tested.

The successful application of these techniques will be applied to the further design of enzyme inhibitors.

Experimental Section

Superimposition of the Active Site of Zinc Metalloprotease Crystal Structures. Four crystal structures were used to construct the superimposition shown on Figure 1: the thermolysin structure 4TMN,⁴⁶ the collagenase structure 1CGL,³⁰ the matrilysin structure 1MMQ,³⁶ and the carboxypeptidase structure 7CPA.⁴⁷ The relevant atoms of the 1MMQ structure were obtained directly from the X-ray crystallographer, Dr. Browner. The remaining structures came from the Brookhaven Data Bank.^{96,97}

Using the MACROMODEL⁶² interactive molecular modeling program, the following atoms were superimposed: the zinc, His 222, and His 218 of collagenase were superimposed on the zinc, His 142 and His 146 of thermolysin; zinc, His 206, and His 218 of matrilysin were superimposed onto the zinc His 142 and His 146 of thermolysin; zinc, inhibitor phosphorus, and ND1 and CE1 of His 196 of carboxypeptidase A onto the zinc, inhibitor phosphorous, and ND1 and CE1 of His 142 of thermolysin.

Construction of an ACE Inhibitor Template. The following compounds were used to construct a template for ACE inhibitors: captopril (**11**),⁵⁶ octahydropyridazo [1,2-*a*]pyrazinediones (**12**),⁸⁷ 2-mercaptocyclohexanecarbonyl-Ala-Pro (**13**),⁸¹ and benazeprilat (**14**)⁵⁵ (see Figure 3).

The crystal structures of captopril⁶³ and benazepril⁶⁴ served as a starting point for the construction of these two molecules. Molecule **12** was constructed using MACROMODEL.⁶² A conformation was generated which matches a picture of the crystal structure of that compound shown in the paper of Hassall.⁸⁷ Molecule **13** was constructed from the crystal structure of captopril. The cyclohexane ring was added with MACROMODEL using the stereochemistry published by Weller.⁸¹

A zinc atom was added to the sulfur of molecules **11–13** and to the carboxylic acid of molecule **14**. A bond length of 2.3 Å was used for the zinc–sulfur bond based on small molecule crystal structures of relevant compounds from Cambridge Structural Database given by Hausin and Coddling.⁶⁵ They reported that the zinc–sulfur–carbon bond angle was found to vary between 91.4° and 104.8° in the crystal structure of small molecules. Therefore, we chose the value of 100°. In the crystal structures of the thiorphan/thermolysin and retro-thiorphan/thermolysin complexes, this bond angle was found to be 124°, whereas in the α -thiol **18**/thermolysin complex structure reported in this work, this bond angle was found to be 99°, indicating that some variability in zinc–sulfur–carbon bond angle is likely upon binding to the enzyme. During the flexible fitting process, all bond angles are allowed small variations according to the AMBER force field and additional parameters added for the interactions between zinc and zinc binding groups.⁹⁸

The geometry for the zinc-carboxylic acid interaction were based on X-ray diffraction data of zinc metalloprotease/inhibitors. Since all of the enzyme/inhibitor structures show the carboxylic acid to bind to zinc in a bidentate manner, this orientation of the oxygens was used for the template. Table 1 gives the bond lengths between the oxygens of the carboxylic acid zinc binding group and the zinc from different X-ray structures. The bond lengths from two other structures were also included: carboxypeptidase complexed with the ligand Bz-Phe⁹⁹ and the “potato” inhibitor.¹⁰⁰ The distances between the zinc and the two carboxylate atoms were 2.2 and 2.7 for the Bz-Phe ligand and 1.8 and 3.2 for the “potato” inhibitor.⁵⁴ The average values of 2.1 and 2.6 Å was, therefore, taken for the zinc–oxygen distances for benazeprilat and all other molecules with the zinc binding carboxylate moiety.

After the addition of the zinc atom, the molecules were minimized using the AMBER force field.¹⁰¹ Adjustments were made to restore the zinc geometry as described above.

To make a composite ACE inhibitor template, low-energy conformations of each molecule were sought which allow the superimposition of the four molecules so that the chemically equivalent atoms occupy the same location. The computer program, TFIND,⁶⁶ was used to identify these conformations. The output of TFIND is a set of superimposed molecules.

TFIND and TFIT. Template making and template fitting were performed using a program called QXP (quick explore).^{66,67} This program has been developed to rapidly perform conformational searches. It carries out conformational explorations in torsion space and has a rapid energy minimizer, which works in torsion space, as well as a fast Cartesian energy minimizer. The program uses application scripts which define a sequence of operations which are performed on the submitted molecular structure. The application scripts for template making is called TFIND and that for template fitting is TFIT.

For template making and template fitting the program uses an extended force field potential which includes a superposition energy. When superposition energy is switched on, atoms which are close to each other in space and of similar chemical type but belong to different molecules receive an attractive potential which forces them to superimpose. Atoms are typed according to hydrophobicity, hydrogen bonding character, and formal charge.

The internal energies of the molecules are also computed, but the normal van der Waals and electrostatic intermolecular energies are switched off. The searches of TFIND, therefore, result in structures

(96) Bernstein, F. C.; Koetzle, T. F.; Williams, G. J. B.; Meyer, E. F.; Brice, M. D.; Rodgers, J. R.; Kennard, T.; Shinamouchi, T.; Tasumi, M. *J. Mol. Biol.* **1977**, *112*, 535–542.

(97) Abol, E. E.; Bernstein, F. C.; Bryant, S. H.; Koetzle, T. F.; Weng, J. In *Crystallographic Databases-Information Content, Software Systems, Scientific Applications*; Allen, F. H., Bergerhoff, G., Sievers, R., Eds.; Data Commission of the International Union of Crystallography: Bonn/Cambridge/Chester, 1987; pp 107–132.

(98) Guida, W. C.; Bohacek, R. S.; Erion, M. D. *J. Comput. Chem.* **1992**, *13*, 214–228.

(99) Christianson, D. W.; Lipscomb, W. N. *J. Am. Chem. Soc.* **1987**, *109*, 5536–5538.

(100) Rees, D. C.; Lipscomb, W. N. *J. Mol. Biol.* **1982**, *160*, 475–498.

(101) Weiner, S. J.; Kollman, P. A.; Case, D. A.; Singh, U. C.; Ghio, C.; Alagona, G.; Profeta, S.; Weiner, P. K. *J. Am. Chem. Soc.* **1984**, *106*, 765–784.

of low internal strain energy which are aligned to optimize the match between atoms.

For template finding, several molecules are submitted. All the molecules are allowed to translate, rotate, and alter their conformations in torsion space. Various conformations of the cyclic parts of the molecules are also generated.

TFIT is used once a proposed template or pharmacophore has been found. The template is kept fixed, and a single test molecule is fitted to it using the superimposition plus internal energy as a guide. TFIT explores the fit of different conformations of cyclic molecules by generating a set of low-energy conformations (Monte Carlo search with internal energy minimization) and then fitting all the conformations using torsional, rotational, and transitional degrees of freedom.

The output of TFIT is a set of superimposed molecules. Several parameters are also reported. The most important is the cost in energy required of the test compound to form the superimposition conformation. This is approximated by taking the difference between the energy of the superimposition conformation and the global minimum internal energy of the compound in vacuum. Another parameter reported by TFIT is the superimposition energy. This energy is a measure of the match between the test compound and the template. It is defined so that when an atom of the ligand approaches an atom of the template, an attractive force is experienced. The superimposition energy reaches a minimum value when two atoms of the same type are superimposed. This term is a useful measure for comparing the degree of superimposition that test compounds with closely similar structures can achieve.

Modeling of Compounds in Thermolysin. A model of the binding site of thermolysin was constructed using the crystal structure of Cbz-Gly^P-Leu-Leu ("Gly^P" = NHCH₂PO₂⁻) bound with thermolysin.⁴⁶ The structure, labeled 5TMN, was obtained from the Brookhaven Protein Data Bank.^{96,97} Only those binding site residues which are near the inhibitors were included in the calculation. The following residues were included: Asn¹¹¹, Asn¹¹², Ala¹¹³, Phe¹¹⁴, Trp¹¹⁵, Asn¹¹⁶, Gly¹¹⁸, Ser¹¹⁸, Gly¹¹⁹, Met¹²⁰, Val¹²¹, Tyr¹²², Gly¹²³, Phe¹³⁰, Leu¹³³, Asp¹³⁸, Val¹³⁹, Val¹⁴⁰, Ala¹⁴¹, His¹⁴², His¹⁴³, His¹⁴⁶, Tyr¹⁵⁷, Ser¹⁶⁹, Asp¹⁸⁰, Glu¹⁶⁵, Glu¹⁶⁶, Ile¹⁸⁸, Gly¹⁸⁹, Gly¹⁹⁰, Val¹⁹², Tyr¹⁹³, Leu²⁰², Arg²⁰³, Asp²²⁶, Val²²⁷, Val²³⁰, His²³¹, and Val²³².

It is known from the crystal structures of different inhibitors bound to thermolysin that there is not a great deal of movement of the enzyme atoms upon binding with different inhibitors. Several residues have been found to display small changes in their conformation with the different inhibitors. To include this enzyme flexibility in our model, residues which displayed the most movement were allowed to move freely during the energy minimization step. Residues found near the inhibitor that show smaller amounts of movement were constrained only by small amounts, i.e., 0.5 and 1.0 kJ. The remaining residues which form a shell around the more flexible residues were constrained with a force constant of 500.0 kJ.

To determine if a molecule can fit into the active site of thermolysin, each molecule was constructed using the interactive molecular modeling program, MACROMODEL.⁶² The conformation of thiorphan from the thiorphan/thermolysin crystal structure served as a starting point. The sulfur atom was bound to the zinc with a zero order bond. The structure was then energy minimized using the AMBER force field¹⁰¹ as implemented by the QXP program.⁶⁶ The Monte Carlo/energy minimization protocol of the MCDOCK module of the QXP program was used with 150 search and energy minimization cycles resulting in a thorough conformational search assuring the exploration of a variety of different binding modes. Previous work using the BATCHMIN⁶² program of MACROMODEL describes the binding site model and gives the parameters used for the zinc-sulfur geometry.⁹⁸

After energy minimization within the active site, a conformational search was conducted to determine the lowest energy conformation of the molecule in the absence of the enzyme. The difference between the energy of the bound conformation and the energy of the conformation minimized outside the binding sites was taken as a measure of the ligand strain energy. A ligand strain energy above 25 kJ is taken to be excessively high indicating that the bound conformation is not energetically accessible to that molecule.

The total energy between the ligand and the binding site atoms is also reported. This energy is defined as the sum of the interaction energy, the enzyme strain energy, and ligand strain energies. The

Table 5. Crystallographic and Stereochemical Parameters of the Refined Structure of Thermolysin Complexed with the Inhibitor **11**

resolution	6.0–1.9 Å
no. of reflections	20236
<i>R</i> -factor	0.156
RMSD	
bond lengths	0.013 Å
bond angles	2.26 deg
dihedral angles	23.0 deg
non-hydrogen atoms in structure	
thermolysin	2432
inhibitor CGS 28106	29
calcium ions	4
zinc atom	1
1 DMSO molecule	4
water molecules	241
total	2711

interaction energy is the sum of the van der Waals energy, electrostatic energy, and an approximate term for hydrophobic attraction between the enzyme and the ligand.⁶⁶ Although we have not found a quantitative correlation between the total energy and experimental binding affinities, this energy has been found to be useful in a qualitative way to distinguish between the ligands which form good interactions with the binding site and those that cannot.

The final steps of the evaluation of a docked structure is visual. After conformational searching and energy minimization in the binding site, the structures are scrutinized to determine if they can form the hydrogen bonds and hydrophobic interactions known to occur in the thermolysin/inhibitor crystal structures of similar inhibitors.

X-ray Crystallography. Thermolysin (Merck, Darmstadt) was crystallized according to the procedure of Matthews et al.¹⁰² Crystals were stored in a mother liquor composed of 0.01 M calcium acetate, 0.01 M tris acetate, and 5% (v/v) dimethyl sulfoxide, pH 7.2. Native crystals were soaked in the same mother liquor containing approximately 7 mM of compound **18** for 1 h. A single crystal was used to collect data. This procedure was tested by collecting three-dimensional diffraction data with a home X-ray source (Nonius FR 571 generator and FAST area detector). A difference electron density map for data to 2.5 Å resolution provided clear density for the inhibitor. The same soaking procedure was used to prepare a single crystal for data collection at a synchrotron X-ray source. Diffraction data was collected on the wiggler beam line on the synchrotron at the EMBL outstation at the Deutsche Elektronen Synchrotron (DESY) in Hamburg, Germany. A monochromatic beam with a wavelength of 0.875 Å was selected. The detection system was an 18-cm diameter image plate system (MarResearch, Hamburg). The crystal to film distance was 18 cm corresponding to a resolution of 1.8 Å at the edge of the image plate. A large, single crystal of thermolysin into which **18** had been allowed to soak was mounted with the 6-fold symmetry axis roughly parallel to the spindle axis and 40 degrees of diffraction data were collected with a rotation range of 1 degree per plate exposure. Exposure times were dependent on the current beam strength but averaged around 1 min per degree. The images could not be satisfactorily processed on site and were later processed at the Biocentre (Basle) with the XDS processing program of Kabsch.¹⁰³ Reflections with a scaled and merged intensity of less than zero were rejected. Useful data extended to 1.9 Å resolution with an average multiplicity of 3.2 and a completeness of 76.7%. The overall $R_{\text{merge}} (S|I_i - \langle I \rangle) / S I_i$, summed over all symmetrically equivalent reflections) was 8.6% with 35% for the outermost shell (1.95–1.90 Å). The structure of thermolysin from Holmes and Matthews¹⁰⁴ was taken from the Brookhaven Protein Data Bank, accession number 3TLN, since superseded by 8TLN. This structure proved to be isomorphous with our crystal form.

The starting crystallographic *R*-factor ($(S|F_o - F_c|/SF_o)$) was 0.317. Partial refinement of the structure without the inhibitor was carried out using the molecular dynamics refinement program X-PLOR¹⁰⁵ but

(102) Matthews, B. W.; Jansonius, J. N.; Colman, P. M.; Shoeborn, B. P.; Dupouque, D. *Nature New Biol.* **1972**, *238*, 37–41.

(103) Kabsch, W. *J. Appl. Cryst.* **1988**, *21*, 916–924.

(104) Holmes, M. A.; Matthews, B. W. *J. Mol. Biol.* **1982**, *160*, 623–639.

(105) Brunger, A. T.; Kuryan, J.; Karplus, M. *Science* **1987**, *235*, 458–460.

without molecular dynamics. An $F_o - F_c$ difference electron density map showed very clear density for the inhibitor **18**, although the density for the tricyclic moiety of the inhibitor was far less clear than for the rest of the molecule. The inhibitor was built into the structure using FRODO¹⁰⁶ running on an Evan and Sutherland PS390 graphics system. Some water molecules were also found in the structure at this time. A molecule of dimethyl sulfoxide, used for crystallization, was also located. A dictionary entry of stereochemical parameters for X-PLOR for **18** was created, and the protein complexed with the inhibitor was refined using molecular dynamics refinement. Alternating cycles of examination of electron density maps, manual correction of the structure (especially adding solvent molecules) and refinement resulted in a final crystallographic *R*-factor of 15.6% and good stereochemistry (Table 5) according to the bond and angle parameter of Engh and Huber.¹⁰⁷

Acknowledgment. The authors wish to acknowledge Dr. J. Stanton who suggested the original ACE inhibitor composite template and whose suggestions significantly enhanced this manuscript. We thank L. Blanchard and L. Stamford for the

(106) Jones, T. A. *J. Appl. Cryst.* **1978**, *11*, 268–272.

(107) Engh, R. A.; Huber, R. *Acta Crystallogr.* **1991**, *A47*, 392–400.

(108) Tronrud, D. E.; Holden, H. M.; Matthews, B. W. *Science* **1987**, *235*, 571–574.

(109) Kim, H., Lipscomb, W. N. *Biochemistry* **1990**, *29*, 5546–5555.

(110) Mangani, S.; Carloni, P.; Orioli, P. *J. Mol. Biol.* **1992**, *223*, 573–578.

synthesis of **10** and **18**. We also wish to gratefully acknowledge Dr. R. D. Ghai, Y. Sakane, and C. Berry who performed the biological assays and Dr. C. G. Paris who did database searching for geometrical parameters of zinc binding ligands. We would like to thank J. Rahuel for technical assistance in crystallization. We would also like to express our appreciation to Ch. Betzel and his colleagues at the EMBL outstation at DESY, Hamburg for their help in synchrotron data collection and to Drs. J. N. Jansonius, T. Schemer, and co-workers at the Biocentre in Basel for their aid in processing this data. We thank Dr. Michelle Browner of Syntex for sending us the coordinates of the atoms near the catalytic zinc from a matrylisin/inhibitor complex prior to the Brookhaven release of this structure. The suggestions and comments of Drs. G. Ksander, Yangbo Ding, and Bryan Marten concerning this manuscript are also gratefully acknowledged.

Supporting Information Available: Synthetic procedures and characterization of **18** (3 pages). See any masthead page for ordering information and Internet access instructions. The X-ray coordinates of the complex of thermolysin with **18** (CGS 28106) will be deposited in the Brookhaven Protein Data Bank.

JA950818Y